Title
Limited cross-variant immunity from SARS-CoV-2 Omicron without vaccination

Journal
Nature, 607(7918)

ISSN
0028-0836

Authors
Suryawanshi, Rahul K
Chen, Irene P
Ma, Tongcui
et al.

Publication Date
2022-07-14

DOI
10.1038/s41586-022-04865-0

Peer reviewed

Article

Limited cross-variant immunity from SARS-CoV-2 Omicron without vaccination

https://doi.org/10.1038/s41586-022-04865-0

Received: 13 January 2022

Accepted: 12 May 2022

Published online: 18 May 2022

Open access

Check for updates

Rahul K. Suryawanshi[1,22], Irene P. Chen[1,2,3,4,22], Tongcui Ma[1,5,22], Abdullah M. Syed[1,6], Noah Brazer[7], Prachi Saldhi[7], Camille R. Simoneau[1,3,4], Alison Ciling[1,6], Mir M. Khalid[1], Bharath Sreekumar[1], Pei-Yi Chen[1], G. Renuka Kumar[1], Mauricio Montano[1,8], Ronne Gascon[1], Chia-Lin Tsou[1], Miguel A. Garcia-Knight[9], Alicia Sotomayor-Gonzalez[7], Venice Servellita[7], Amelia Gliwa[7], Jenny Nguyen[7], Ines Silva[10], Bilal Milbes[10], Noah Kojima[21], Victoria Hess[10], Maria Shacreaw[10], Lauren Lopez[10], Matthew Brobeck[10], Fred Turner[10], Frank W. Soveg[1], Ashley F. George[1,11], Xiaohui Fang[12,13], Mazharul Maishan[12,13], Michael Matthay[12,13], Mary Kate Morris[14], Debra Wadford[14], Carl Hanson[14], Warner C. Greene[1,3,8,9], Raul Andino[9], Lee Spraggon[10], Nadia R. Roan[1,11] ✉, Charles Y. Chiu[3,5,6,7,15] ✉, Jennifer A. Doudna[1,6,16,17,18,19,20] ✉ & Melanie Ott[1,3,4,15] ✉

SARS-CoV-2 Delta and Omicron are globally relevant variants of concern. Although individuals infected with Delta are at risk of developing severe lung disease, infection with Omicron often causes milder symptoms, especially in vaccinated individuals[1,2]. The question arises of whether widespread Omicron infections could lead to future cross-variant protection, accelerating the end of the pandemic. Here we show that without vaccination, infection with Omicron induces a limited humoral immune response in mice and humans. Sera from mice overexpressing the human ACE2 receptor and infected with Omicron neutralize only Omicron, but not other variants of concern, whereas broader cross-variant neutralization was observed after WA1 and Delta infections. Unlike WA1 and Delta, Omicron replicates to low levels in the lungs and brains of infected animals, leading to mild disease with reduced expression of pro-inflammatory cytokines and diminished activation of lung-resident T cells. Sera from individuals who were unvaccinated and infected with Omicron show the same limited neutralization of only Omicron itself. By contrast, Omicron breakthrough infections induce overall higher neutralization titres against all variants of concern. Our results demonstrate that Omicron infection enhances pre-existing immunity elicited by vaccines but, on its own, may not confer broad protection against non-Omicron variants in unvaccinated individuals.

Since the beginning of the COVID-19 pandemic, multiple waves of infection have occurred from SARS-CoV-2 variants of concern (VOCs) that continue to arise and out-compete preceding variants. VOCs with worldwide relevance are Delta (B.1.617.2) and most recently Omicron (BA.1), whereas Alpha (B.1.1.7), Beta (B.1.351) and Gamma (P.1) variants spread more locally. Compared to the ancestral isolate (WA1 or B.1), Omicron is characterized by a large number of unique mutations in the spike protein as well as in other structural proteins, select non-structural proteins and accessory open reading frames. Omicron bears over 50 mutations across its genome, including approximately 37 mutations (28 being unique and nine overlapping with other variants) in the spike glycoprotein, which may contribute to its antigenic differences[3–9].

The constellation of mutations in the Omicron spike protein has been associated with increased transmission[10], decreased spike cleavage[11] and decreased cell-to-cell fusion[11,12]. Omicron spike mutations limit efficacies of neutralizing antibodies generated by previous infections, vaccines and treatment with monoclonal antibodies[3–9,13]. Indeed, the risk of breakthrough infections and re-infections is increased with Omicron[13–15]. However, disease severity is lower with Omicron than with Delta[1,2,13], and

[1]Gladstone Institutes, San Francisco, CA, USA. [2]Biomedical Sciences Graduate Program, University of California, San Francisco, San Francisco, CA, USA. [3]Department of Medicine, University of California, San Francisco, San Francisco, CA, USA. [4]Quantitative Biosciences Institute COVID-19 Research Group, University of California, San Francisco, San Francisco, CA, USA. [5]UCSF-Abbott Viral Diagnostics and Discovery Center, San Francisco, CA, USA. [6]Innovative Genomics Institute, University of California, Berkeley, Berkeley, CA, USA. [7]Department of Laboratory Medicine, University of California, San Francisco, San Francisco, CA, USA. [8]Michael Hulton Center for HIV Cure Research at Gladstone, San Francisco, CA, USA. [9]Department of Microbiology and Immunology, University of California, San Francisco, San Francisco, CA, USA. [10]Curative Inc., San Dimas, CA, USA. [11]Department of Urology, University of California, San Francisco, San Francisco, CA, USA. [12]Department of Medicine, Cardiovascular Research Institute, University of California, San Francisco, San Francisco, CA, USA. [13]Department of Anesthesia, Cardiovascular Research Institute, University of California, San Francisco, San Francisco, CA, USA. [14]California Department of Public Health, Richmond, CA, USA. [15]Chan Zuckerberg Biohub, San Francisco, CA, USA. [16]Department of Molecular and Cell Biology, University of California, Berkeley, Berkeley, CA, USA. [17]Molecular Biophysics and Integrated Bioimaging Division, Lawrence Berkeley National Laboratory, Berkeley, CA, USA. [18]Howard Hughes Medical Institute, University of California, Berkeley, Berkeley, CA, USA. [19]Department of Chemistry, University of California, Berkeley, Berkeley, CA, USA. [20]California Institute for Quantitative Biosciences, University of California, Berkeley, Berkeley, CA, USA. [21]Department of Medicine, University of California, Los Angeles, Los Angeles, CA, USA. [22]These authors contributed equally: Rahul K. Suryawanshi, Irene P. Chen, Tongcui Ma. ✉e-mail: nadia.roan@gladstone.ucsf.edu; charles.chiu@ucsf.edu; doudna@berkeley.edu; melanie.ott@gladstone.ucsf.edu

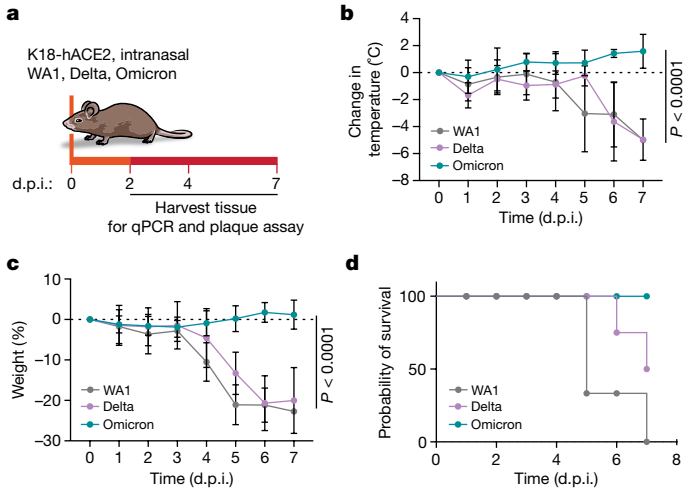

Fig. 1 | Robust infection of K18-hACE2 mice with the Delta and ancestral variants, but not with the Omicron variant. a, Schematic of the experiment. Fifteen mice per group were intranasally infected with 10^4 p.f.u. of the indicated variant. Body temperature and weight were monitored daily. At 2, 4 and 7 days post-infection (d.p.i.), the upper respiratory tract and lungs were harvested and processed for downstream analysis. $n = 5$ per group. **b**, Changes in body temperature of mice infected with WA1, Delta and Omicron. Data are shown as the average ± s.d. and were analysed by two-way analysis of variance (ANOVA) and adjusted for multiple testing using the Bonferroni test. **c**, Severe weight loss of WA1-infected and Delta-infected mice. Data are shown as the average ± s.d. and were analysed by two-way ANOVA and adjusted for multiple testing using the Bonferroni test. The horizontal dashed lines in **b**,**c** indicate the baseline body temperature (**b**) and weight (**c**) of mice. **d**, Probability of survival of variant-infected mice. $n = 10$.

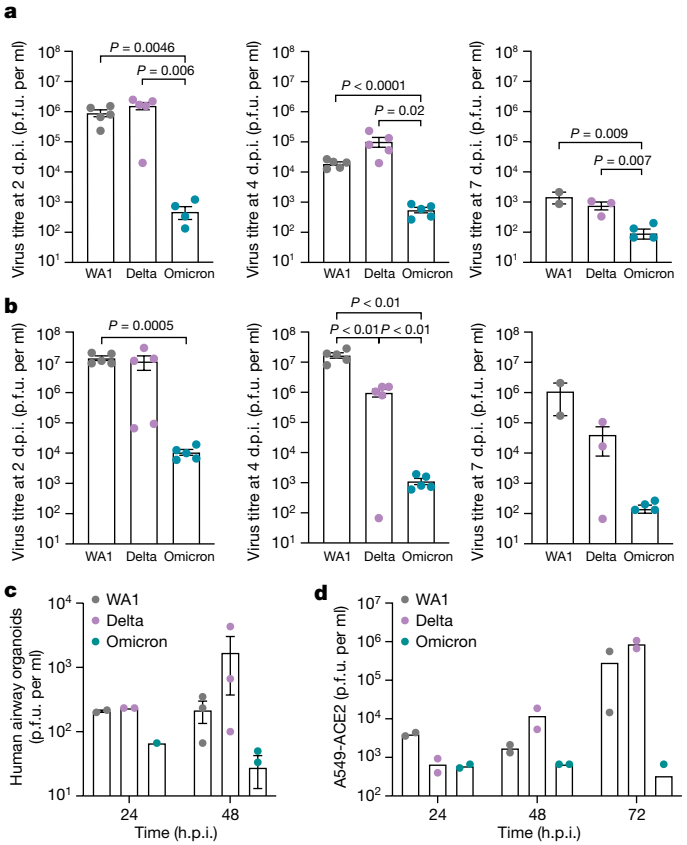

Fig. 2 | Robust viral replication of WA1 and Delta, but not Omicron, in airway cells from mice and humans. a, Plaque assay titres from the upper airway (nasal turbinates and bronchus) of WA1-infected, Delta-infected and Omicron-infected mice at the indicated time points. Data are shown as the average ± s.e.m. analysed by the two-tailed unpaired Student's *t*-test. Each dot represents an infectious virus titre in an individual mouse at 2 d.p.i. ($n = 5$), 4 d.p.i. ($n = 5$) and 7 d.p.i. (WA1 infection group $n = 2$, Delta $n = 2$ and Omicron $n = 5$). **b**, Plaque assay titres from the lungs of infected mice at the indicated time points. Data are shown as the average ± s.e.m. at each time point and were analysed by the two-tailed unpaired Student's *t*-test. Each dot represents infectious virus titre in individual mice at 2 d.p.i. ($n = 5$), 4 d.p.i. ($n = 5$) and 7 d.p.i. (WA1 infection group $n = 2$, Delta $n = 2$ and Omicron $n = 5$). **c**, Plaque assay titres from supernatants of infected human airway organoids (multiplicity of infection (MOI) of 1). Data are shown as the average ± s.e.m. Each dot represents an independent experiment using human lung airway organoids generated at 24 h ($n = 2$) and 48 h ($n = 3$). h.p.i., hours post-infection. **d**, Plaque assay titres from supernatants of infected A549-ACE2 cells (MOI of 0.1). $n = 2$ represents infectious virus titres in independent experiments.

previous infection or vaccination reduces the risk of hospitalization with Omicron[16,17]. Pressing questions are how effective Omicron-induced immunity is and whether it is cross-protective against other variants.

Omicron causes less severe infection

To answer these questions, we studied WA1, Delta and Omicron infections in mice. Because WA1 and Delta variants cannot infect regular laboratory mice[18], we used transgenic mice overexpressing human ACE2 (K18-hACE2)[19]. We intranasally infected (10^4 plague-forming units (p.f.u.)) these mice with the three viral isolates, and over 7 days monitored their body temperature and weight, which serve as indicators of disease progression (Fig. 1a). Although Delta-infected and WA1-infected mice showed progressive hypothermia and severe weight loss during this time, Omicron-infected mice exhibited very mild symptoms with only a small increase in body temperature and no weight loss (Fig. 1b,c). Five days after infection, the WA1-infected and Delta-infected mice were hunched or lethargic, but the Omicron-infected mice appeared completely normal (Extended Data Fig. 1a). All of the Omicron-infected mice survived the 1-week experiment; yet, 100% of the WA1-infected and 60% of the Delta-infected animals reached the humane end point during this time (Fig. 1d). This replicates previous findings from infected individuals, mice and hamsters that have shown mild disease with Omicron infection, but not with Delta and WA1 infections[1,2,20–24].

To assess viral replication dynamics, we quantified infectious particle production (Fig. 2a,b) and viral RNA expression (Extended Data Fig. 2a,b) in the respiratory tracts and lungs of infected mice over time. Across all time points, high titres of infectious virus were present in the upper airways (nasal turbinates and bronchi) and lungs of WA1-infected and Delta-infected mice, whereas Omicron replication was significantly lower in these organs, as previously reported[20–22]. Lung histology showed that Omicron infection resulted in small localized foci of infected cells (marked by nucleocapsid staining (green)) (Extended Data Fig. 1b–d). A similar pattern but with enhanced numbers were observed after WA1 infection, and Delta infection showed large patches of infected cells, indicative of enhanced cell-to-cell spread, as reported in human lung organoids and cell lines[11] (Extended Data Fig. 1b–d). In addition, brain tissue, which is a target for viral replication in K18-hACE2 mice, showed lower Omicron replication 4 and 7 days after infection. Omicron infection also produced fewer infectious particles in human airway organoids and the human alveolar A549 epithelial cell line overexpressing ACE2 than WA1 and Delta infections (Fig. 2c,d), which is consistent with our findings in mice.

Immune markers differ between variants

As severe COVID-19 is associated with cytokine storms in conjunction with exhaustion of T cells[25], we next assessed cytokine expression and T cell phenotypes in infected mouse lungs. Although infection with

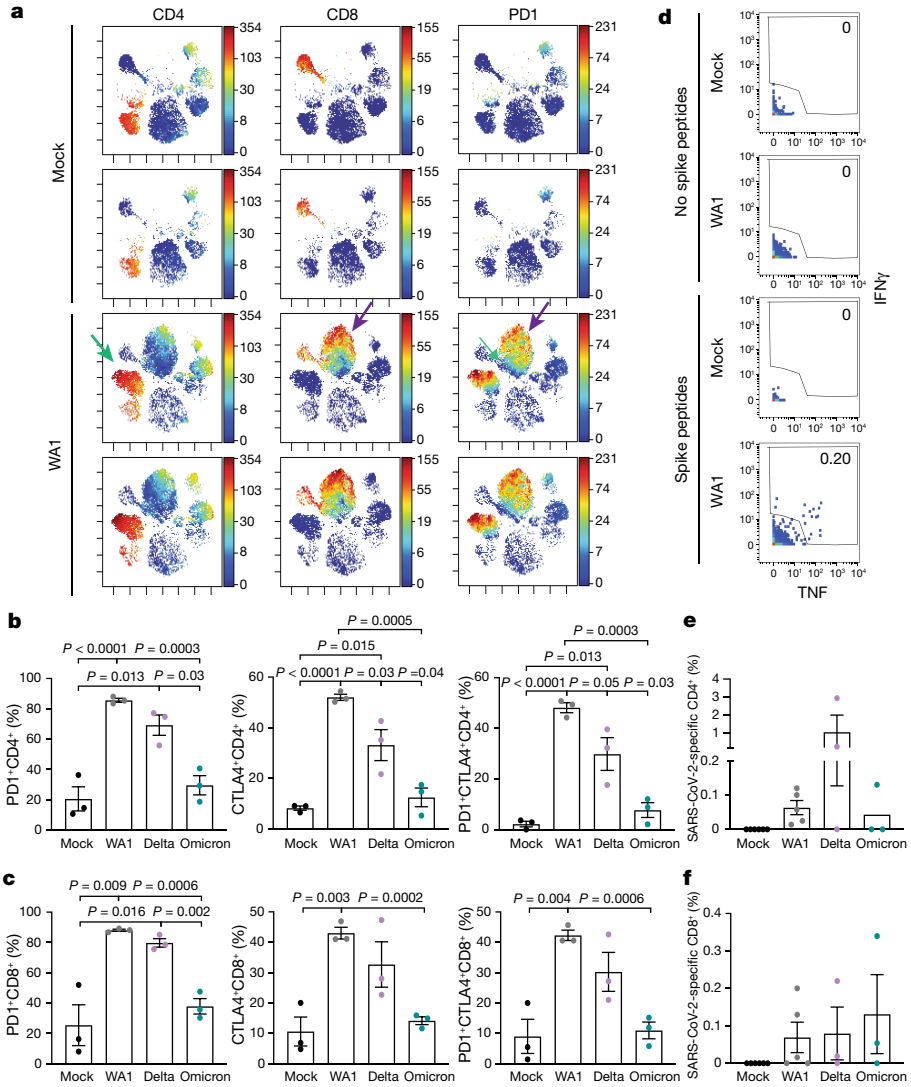

Fig. 3 | Ancestral and VOC SARS-CoV-2 elicit immune responses in the lungs of mice. a, T cells from lungs of infected mice ($n = 3$) were phenotypically distinct and expressed PD1. Single-cell suspensions of lungs from mock-infected and WA1-infected K18-hACE2 mice were harvested at 9 d.p.i. and analysed by CyTOF. Shown are tSNE plots gated on total immune cells ($CD45^+$) from the lungs of mice, coloured by expression levels of the antigen listed at the top (red shows the highest expression and blue represents the lowest expression). 'Islands' of $CD4^+$ and $CD8^+$ T cells unique to the infected mice (identified by green and purple arrows, respectively, in the third row) express especially high levels of the activation/exhaustion marker PD1, as demonstrated in the right-hand column. **b**,**c**, T cells from lungs of infected mice ($n = 3$) expressed elevated levels of the activation/checkpoint antigens PD1 and CTLA4. The proportions of $CD4^+$ (**b**) and $CD8^+$ (**c**) T cells expressing PD1, CTLA4 or both PD1 and CTLA4 are indicated. **d**, SARS-CoV-2-specific T cells are elicited in the lungs of mice infected with SARS-CoV-2. Representative plots corresponding to pulmonary T cells from uninfected (mock) and WA1-infected K18-hACE2 mice, stimulated for 6 h with or without overlapping SARS-CoV-2 spike peptides. Note that SARS-CoV-2-specific T cells (those producing IFNγ and/or TNF) were only detected in infected mice after peptide stimulation ($n = 3$). **e**,**f**, SARS-CoV-2-specific T cells are elicited in the lungs of mice infected with WA1 ($n = 6$), Delta ($n = 3$) and Omicron ($n = 3$). The proportions of $CD4^+$ (**e**) and $CD8^+$ (**f**) T cells expressing IFNγ and/or TNF (gated as shown in **c**) are indicated. $CD4^+$ T cell responses trended highest in Delta-infected mice, and the $CD8^+$ T cell responses were highest in Delta-infected and Omicron-infected mice ($n = 3$). In **b**,**c**,**e**,**f**, data are shown as the average ± s.e.m. analysed by the two-tailed unpaired Student's *t*-test.

WA1 and Delta readily induced pro-inflammatory markers of severe COVID, such as CXCL10 and CCL2 (ref. [26]), induction by Omicron was significantly reduced early after infection (Extended Data Fig. 3a). Induction of IL-1α was not significantly different between the three viral isolates, but trended towards lower expression in Omicron-infected animals 2 days post-infection (Extended Data Fig. 3a). Although no significant differences between the viral variants were observed in the induction of IFNα or relevant downstream induced genes, such as interferon-stimulated gene 15 (*ISG15*) and 2'-5'-oligoadenylate synthetase 1 (*OAS1*), we cannot exclude that this is caused by a low number of animals at later time points (Extended Data Fig. 3a,b).

To determine whether the pro-inflammatory response that we observed in WA1-infected mice is also associated with T cell exhaustion in late infection, we generated single-cell suspensions from the lungs of mock-infected and WA1-infected mice, and performed cytometry by time of flight (CyTOF) mass spectrometry before and after stimulation with overlapping 15-mer peptides that span the entire spike protein. tSNE visualization of the CyTOF data corresponding to total immune ($CD45^+$) cells from the unstimulated specimens revealed that both $CD4^+$ and $CD8^+$ T cells of infected mice segregate distinctly from their respective counterparts in the mock-infected mice, indicating profound phenotypic changes in pulmonary T cells upon WA1 infection, including upregulation of the

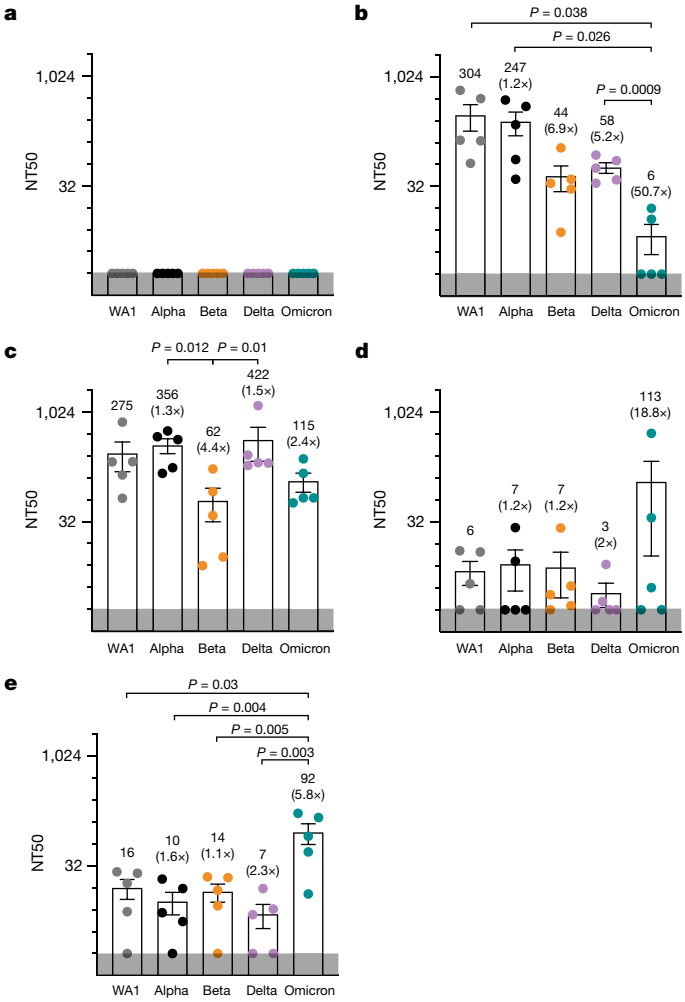

Fig. 4 | Cross-variant neutralization of SARS-CoV-2 isolates from the sera of infected mice. K18-hACE2 mice were infected with 1×10^4 p.f.u. of WA1, Delta or Omicron. The virus neutralization assay was carried out with sera collected at 7 d.p.i. Data points in the graph represent individual sera samples showing NT50s against SARS-CoV-2 isolates. The numbers in parentheses indicate the fold change in neutralization efficacy or resistance of respective isolates relative to the NT50 of the ancestral isolate (WA1). The grey band at the bottom of the graph indicates the limit of detection. **a**–**d**, Graphs representing the NT50 of sera from naive (**a**), WA1-infected (**b**), Delta-infected (**c**) and Omicron-infected (**d**) mice against different viral isolates. $n = 5$ mouse in each group. **e**, K18-hACE2 mice were infected with 5×10^2 p.f.u. of Omicron ($n = 5$). The virus neutralization assay was carried out with sera collected at 9 d.p.i. Data are presented as average ± s.e.m. and were analysed by two-way ANOVA and two-tailed unpaired Student's *t*-test.

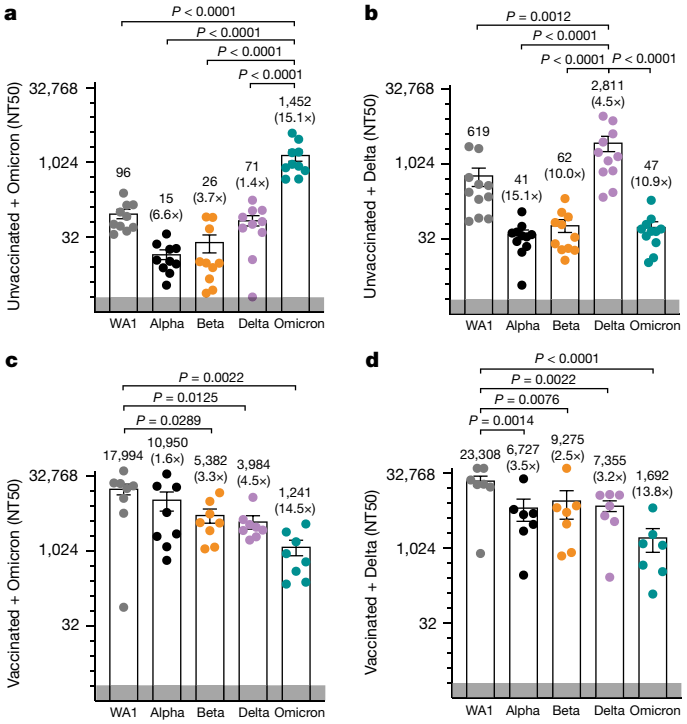

Fig. 5 | Cross-variant neutralization of SARS-CoV-2 isolates from human sera. a–**d**, Graphs representing the NT50 of variants by sera from unvaccinated individuals with likely Omicron infection (based on date of collection; $n = 10$) (**a**), unvaccinated individuals with likely Delta infection (based on date of collection; $n = 11$) (**b**), vaccinated individuals with a confirmed Omicron infection ($n = 8$) (**c**) and vaccinated individuals with confirmed Delta infection (based on date of collection; $n = 7$) (**d**). The data points in the graph represent individual serum samples. The grey band at the bottom of the graph indicates the limit of detection. Data presented in a–d are average ± s.e.m. and were analysed by two-way ANOVA and two-tailed unpaired Student's *t*-test. The details regarding samples (group, age, sex, COVID-19 infection status, vaccination dates, and sample collection dates after infection or symptoms are summarized in Extended Data Table 1).

activation/exhaustion marker programmed cell death 1 (PD1) on T cells from the infected animals (Fig. 3a).

When similar experiments were performed with infections by WA1, Delta and Omicron, we found elevated expression levels of not only PD1 but also cytotoxic T lymphocyte-associated protein 4 (CTLA4; which is another activation/exhaustion marker) on pulmonary T cells in all infected animals, although to a significantly lesser extent in the Omicron-infected mice (Fig. 3b,c). Despite evidence of pulmonary T cell exhaustion in mice infected with all three isolates, functional SARS-CoV-2-specific T cells were still generated in the lungs, as demonstrated by our identification of IFNγ-producing and TNF-producing cells specifically in the peptide-stimulated specimens (Fig. 3d–f). These results suggest that the diminished pro-inflammatory cytokines and activated/exhausted pulmonary T cells elicited by Omicron associate with diminished Omicron pathogenicity and the 2–3 logs decrease in Omicron replication.

Cross-variant neutralization

To determine humoral immune responses induced by infection with the three different isolates, we collected sera from mice at 7 days after infection and tested their neutralization efficiency against SARS-CoV-2 isolates: WA1, Alpha, Beta, Delta and Omicron. We determined the p.f.u. at different serum dilutions and calculated the 50% neutralization titres (NT50s) (Fig. 4 and Extended Data Fig. 5). As expected, sera from uninfected mice showed no neutralization across all variants (Fig. 4a). Sera from WA1-infected mice showed effective neutralization of WA1 and Alpha and, to a lesser extent, Beta and Delta isolates, but no efficacy against Omicron (NT50 of 6) (Fig. 4b). By contrast, sera from Delta-infected mice effectively neutralized Delta (NT50 of 422), WA-1 (NT50 of 275), Alpha (NT50 of 356) and, to a lesser extent, Omicron (NT50 of 115) and Beta (NT50 of 62), with the latter significantly decreased, compared to Delta and Alpha (Fig. 4c). Omicron infection, however, only induced neutralization of Omicron (NT50 of 113), but no other isolate (NT50 of 3–7) (Fig. 4d). This was repeated and confirmed in a second experiment in which 9 days after infection, all mice infected with Omicron showed significant serum neutralization of Omicron (NT50 of 92), but no other VOC (NT50 of 7–16) (Fig. 4e). These results indicate

limited cross-variant neutralization induced by Omicron relative to other isolates, which may be due to its highly mutated spike protein or its lower replicative capacity (Fig. 2). Delta and WA1, despite having similar replicative and inflammatory capacities, exhibited different neutralization profiles, underscoring the role of the different spike (and possibly other viral) proteins in eliciting cross-variant neutralization.

These data were confirmed with sera from 10 unvaccinated individuals who had recovered from Omicron infection (Extended Data Table 1). These sera showed the same limited cross-variant neutralization as observed in mice with effective neutralization of only Omicron itself (NT50 of 1,452) and an approximately 15-fold decrease in neutralizing titres against non-Omicron isolates (NT50 of 15–96) (Fig. 5a and Extended Data Fig. 6). Analysis of sera from 11 matched, unvaccinated individuals with Delta infection showed a similar pattern: highest neutralization of Delta itself (NT50 of 2,811), followed by WA1 (NT50 of 619) and decreased neutralization of Alpha, Beta and Omicron (NT50 of 41–62) (Fig. 5b and Extended Data Fig. 7). Sera from uninfected, unvaccinated individuals showed no neutralization across all variants as expected (Extended Data Fig. 4a).

Sera from vaccinated individuals with confirmed Omicron or Delta breakthrough infections showed high neutralizing titres against all isolates, with highest titres against WA1 (NT50 of 17,994 and 23,308) and lowest against Omicron (NT50 of 1,241 and 1,692) (Fig. 5c,d). These values exceeded neutralizing titres induced by the third shot of Pfizer/BioNTech vaccines, in which titres were, on average, 10 times lower than those observed after breakthrough infections (Extended Data Figs. 4b and 8). These results suggest that Omicron and Delta breakthrough infections can boost existing immunity conferred by vaccination, thereby eliciting a form of 'hybrid immunity' that is effective against not only itself but also other SARS-CoV-2 variants.

Collectively, our study shows that, although the Omicron variant is immunogenic, infection in unvaccinated individuals may not elicit effective cross-neutralizing antibodies to non-Omicron variants. However, in vaccinated individuals, Omicron infection effectively induces immunity against itself and enhances neutralization of other variants. This, together with our finding that Delta infection also elicits broad cross-variant neutralization in vaccinated individuals, supports the inclusion of Omicron-based and Delta-based immunogens in future heterologous or multivalent vaccination strategies for broad protection against variants.

Online content

Any methods, additional references, Nature Research reporting summaries, source data, extended data, supplementary information, acknowledgements, peer review information; details of author contributions and competing interests; and statements of data and code availability are available at https://doi.org/10.1038/s41586-022-04865-0.

1. Sigal, A. Milder disease with Omicron: is it the virus or the pre-existing immunity? *Nat. Rev. Immunol.* **22**, 69–71 (2022).
2. Wolter, N. et al. Early assessment of the clinical severity of the SARS-CoV-2 omicron variant in South Africa: a data linkage study. *Lancet* **399**, 437–446 (2022).
3. Dejnirattisai, W. et al. SARS-CoV-2 Omicron-B.1.1.529 leads to widespread escape from neutralizing antibody responses. *Cell* **185**, 467–484.e15 (2022).
4. Syed, A. M. et al. Omicron mutations enhance infectivity and reduce antibody neutralization of SARS-CoV-2 virus-like particles. Preprint at *medRxiv* https://doi.org/10.1101/2021.12.20.21268048 (2022).
5. Mannar, D. et al. SARS-CoV-2 Omicron variant: antibody evasion and cryo-EM structure of spike protein–ACE2 complex. *Science* **375**, 760–764 (2022).
6. Cao, Y. et al. Omicron escapes the majority of existing SARS-CoV-2 neutralizing antibodies. *Nature* **602**, 657–663 (2021).
7. Van Blargan, L. A. et al. An infectious SARS-CoV-2 B.1.1.529 Omicron virus escapes neutralization by therapeutic monoclonal antibodies. *Nat. Med.* **28**, 490–495 (2022).
8. Hoffmann, M. et al. The Omicron variant is highly resistant against antibody-mediated neutralization: implications for control of the COVID-19 pandemic. *Cell* **185**, 447–456.e11 (2022).
9. Planas, D. et al. Considerable escape of SARS-CoV-2 Omicron to antibody neutralization. *Nature* **602**, 671–675 (2021).
10. Espenhain, L. et al. Epidemiological characterisation of the first 785 SARS-CoV-2 Omicron variant cases in Denmark, December 2021. *Euro Surveill.* **26**, 2101146 (2021).
11. Meng, B. et al. Altered TMPRSS2 usage by SARS-CoV-2 Omicron impacts infectivity and fusogenicity. *Nature* **603**, 706–714 (2022).
12. Suzuki, R. et al. Attenuated fusogenicity and pathogenicity of SARS-CoV-2 Omicron variant. *Nature* **603**, 700–705 (2022).
13. Dejnirattisai, W. et al. Reduced neutralisation of SARS-CoV-2 Omicron B.1.1.529 variant by post-immunisation serum. *Lancet* **399**, 234–236 (2021).
14. Pulliam, J. R. C. et al. Increased risk of SARS-CoV-2 reinfection associated with emergence of Omicron in South Africa. *Science* **376**, 6593 (2022).
15. Miyamoto, S. et al. Vaccination-infection interval determines cross-neutralization potency to SARS-CoV-2 Omicron after breakthrough infection by other variants. *Med* **3**, 249–261.e4 (2022).
16. Ferguson, N., Ghani, A., Hinsley, W. & Volz, E. Report 50—hospitalisation risk for Omicron cases in England. *Imperial College London* https://www.imperial.ac.uk/mrc-global-infectious-disease-analysis/covid-19/report-50-severity-omicron (2021).
17. Public Health England. *SARS-CoV-2 Variants of Concern and Variants Under Investigation in England*. Technical Briefing 12 (Public Health England, 2021).
18. Shuai, H. et al. Emerging SARS-CoV-2 variants expand species tropism to murines. *EBioMedicine* **73**, 103643 (2021).
19. Winkler, E. S. et al. SARS-CoV-2 infection of human ACE2-transgenic mice causes severe lung inflammation and impaired function. *Nat. Immunol.* **21**, 1327–1335 (2020).
20. Bentley, E. G. et al. SARS-CoV-2 Omicron-B.1.1.529 variant leads to less severe disease than Pango B and Delta variants strains in a mouse model of severe COVID-19. Preprint at *bioRxiv* https://doi.org/10.1101/2021.12.26.474085 (2021).
21. Halfmann, P. J. et al. SARS-CoV-2 Omicron virus causes attenuated disease in mice and hamsters. *Nature* **603**, 687–692 (2022).
22. Shuai, H. et al. Attenuated replication and pathogenicity of SARS-CoV-2 B.1.1.529 Omicron. *Nature* **603**, 693–699 (2022).
23. McMahan, K. et al. Reduced pathogenicity of the SARS-CoV-2 Omicron variant in hamsters. *Med* **3**, 262–268.e4 (2022).
24. Abdelnabi, R. et al. The Omicron (B.1.1.529) SARS-CoV-2 variant of concern does not readily infect Syrian hamsters. *Antiviral Res.* **198**, 105253 (2022).
25. Le Bert, N. et al. SARS-CoV-2-specific T cell immunity in cases of COVID-19 and SARS, and uninfected controls. *Nature* **584**, 457–462 (2020).
26. Coperchini, F., Chiovato, L., Croce, L., Magri, F. & Rotondi, M. The cytokine storm in COVID-19: an overview of the involvement of the chemokine/chemokine-receptor system. *Cytokine Growth Factor Rev.* **53**, 25–32 (2020).

Methods

Human lung organoids

Whole human lung tissue was digested to a single-cell suspension and plated in basement membrane extract as previously published[27]. In brief, organoids were maintained in DMEM supplemented with supplemented with 10% (vol/vol) R-spondin1 conditioned medium, 1% B27 (Gibco), 25 ng ml^{-1} noggin (Peprotech), 1.25 mM *N*-acetylcysteine (Sigma-Aldrich), 10 mM nicotinamide (Sigma-Aldrich), 5 nM herefulin-β1 (Peprotech) and 100 μg ml^{-1} Primocin (InvivoGen). HAO medium was further supplemented with 5 μM Y-27632, 500 nM A83-01, 500 nM SB202190, 25 ng ml^{-1} FGF7 and 100 ng ml^{-1} FGF10 (all from Stem Cell Technologies). HAO medium was replaced every 3–4 days.

A549 cells expressing ACE2 (A549-ACE2) from the American Type Culture Collection (ATCC) and Vero cells expressing TMPRSS (Vero-TMPRSS2) were a gift from O. Schwartz and S. P. J. Whelan, respectively. A549-ACE2 and Vero-TMPRSS2 cells were cultured in DMEM supplemented with 10% FBS and blasticidin (20 μg ml^{-1}) (Sigma) at 37 °C and 5% CO_2. Short terminal repeat analysis by the Berkeley Cell Culture Facility authenticated these as A549 cells with 100% probability. The cells are free of mycoplasma contamination.

Vero cells stably co-expressing human ACE2 and TMPRSS2 (a gift from A. Creanga and B. Graham at the US National Institutes of Health) were maintained at 37 °C and 5% CO_2 in DMEM (Gibco) supplemented with 10% fetal calf serum, 100 μg ml^{-1} penicillin and streptomycin (Gibco) and 10 μg ml^{-1} puromycin (Gibco). The cells are free of mycoplasma contamination.

SARS-CoV-2 virus culture

SARS-CoV-2/human/USA/USA-WA1/2020 (WA1) (BEI NR-52281), B.1.1.7 (California Department of Health), B.1.351 (BEI NR-54008), B.1.617.2 (California Department of Health) and B.1.1.529 (California Department of Health; BA.1) were used for animal infection studies or serum virus neutralization. The virus infection experiments were performed in a biosafety level 3 laboratory. Working stocks of SARS-CoV-2 were made in Vero-TMPRSS2 cells and were stored at −80 °C until used.

The Omicron variant was isolated from a nasopharyngeal swab sample from a patient hospitalized with COVID-19 at the University of California, San Francisco (UCSF). A 200 μl aliquot of the sample was serially diluted 1:1 with medium (DMEM supplemented with 1× penicillin–streptomycin) in a 96-well plate for five dilutions, in duplicate. Then, 100 μl of freshly trypsinized Vero-hACE2–TMPRSS2 cells, resuspended in infection medium (made as above but with 2× penicillin–streptomycin, 5 μg ml^{-1} amphotericin B (Bioworld) and no puromycin) were added to the nasal sample dilutions at a concentration of 2.5×10^5 cells per ml. Cells were cultured at 37 °C and 5% CO_2 and checked for cytopathic effects (CPEs) from days 2 to 3. Vero-hACE2–TMPRSS2 cells formed characteristic syncytia upon infection with SARS-CoV-2, enabling rapid and specific visual evaluation for CPEs. Supernatants were harvested on day 3 after inoculation. A 200 μl aliquot of passage 0 (P0) was used to infect a confluent T25 flask to generate a P1 culture, harvested after 3 days. Virus stocks were titred by plaque assay, and the sequence was confirmed by nanopore sequencing.

K18-hACE2 mouse infection model

All protocols concerning animal use were approved (AN169239-01C) by the Institutional Animal Care and Use committees at the University of California, San Francisco and Gladstone Institutes and conducted in strict accordance with the National Institutes of Health Guide for the Care and Use of Laboratory Animal[28]. Mice were housed in a temperature-controlled (65–75 °F) and humidity-controlled (40–60%) pathogen-free facility with a 12-h light–dark cycle and ad libitum access to water and standard laboratory rodent chow.

In brief, the study involved intranasal infection (1×10^4) of 6–8-week-old female K18-hACE2 mice with Delta and Omicron, and WA1 served as a control isolate of SARS-CoV-2. A total of 15 animals were infected for each variant. Five mice from each group were euthanized at 2, 4 and 7 days post-infection. The brain, lungs and upper respiratory tract, including bronchus and nasal turbinates, were processed for further analysis of virus replication.

Cellular infection studies

A549-ACE2 cells were seeded into 12-well plates. Cells were rested for at least 24 h before infection. At the time of infection, medium containing viral inoculum (MOI of 0.01 and 0.1) was added on the cells. At 1 h after addition of inoculum, the medium was replaced with fresh medium without viral inoculum. Supernatants were harvested at 24, 48 and 72 h post-infection for further plaque assays.

Organoid infection studies

Organoids were plated on geltrex-coated plates (12760013, Thermo Fisher) with 100,000 cells per well, and infected at an MOI of 1. At 2 h after addition of the inoculum, the supernatant was removed, cells were washed with PBS and fresh HAO medium was added. Supernatants were harvested for a plaque assay at 24 and 48 h.

Virus neutralization assay

K18-hACE2 mice were infected with 1×10^4 p.f.u. of WA1, B.1.617.2 and B.1.1.529 ($n = 5$). With the early humane end points with WA1 and B.1.617.2, more animals ($n = 15$) were infected for these groups. Serum samples from mice were collected at 7 days post-infection. Mock-infected animals served as controls. Serum dilutions (50 μl) were made to get final dilutions of 1:30, 1:90, 1:270, 1:810, 1:2,430 and 1:7,290 in serum-free DMEM. Dilutions were separately added with 50 p.f.u. (50 μl) of SARS-CoV-2 WA1, Alpha, Beta, Delta and Omicron. The mixture was mixed gently, incubated at 37 °C for 30 mins, followed by a plaque assay. Similar assays were performed for serum samples from Omicron-infected (5×10^2) mice obtained at 9 d.p.i., and human serum samples acquired from ongoing clinical trials led by Curative and the UCSF or from hospitalized patients at the UCSF (Extended Data Table 1). The virus neutralization efficacy of sera was presented as NT50 and the average of each variant, and compared to others in terms of fold change. NT50 graphs were generated by MATLAB (version 9.12). Data analysis was performed by using GraphPad Prism version 9.3.

Plaque assays

Tissue homogenates and cell supernatants were analysed for viral particle formation for in vivo and in vitro experiments, respectively. In brief, Vero-TMPRSS2 cells were seeded and incubated overnight. Cells were inoculated with 10^{-1} to 10^{-6} dilutions of the respective homogenates or supernatant in serum-free DMEM. After the 1-h absorption period, the media in the wells were overlaid with 2.5% Avicel (RC-591, Dupont). After 72 h, the overlay was removed, and the cells were fixed in 10% formalin for 1 h and stained with crystal violet for visualization of p.f.u. Data analysis was performed by using GraphPad Prism version 9.3.

Quantitative PCR

RNA was extracted from cells, supernatants or tissue homogenates with RNA-STAT-60 (CS-110, AMSBIO) and the Direct-Zol RNA Miniprep Kit (R2052, Zymo Research). RNA was then reverse-transcribed to cDNA with iScript cDNA Synthesis Kit (1708890, Bio-Rad). Quantitative PCR was performed with cDNA and SYBR Green Master Mix (Thermo Scientific) using the CFX384 Touch Real-Time PCR Detection System (Bio-Rad). See Extended Data Table 2 for primers sequences. N gene standards were used to generate a standard curve for copy number quantification. N gene standard was generated by PCR using extracted genomic SARS-CoV-2 RNA as template. A single product was confirmed by gel electrophoresis, and DNA was quantified by Nanodrop.

CyTOF analysis of mouse lung specimens

The mice used in the CyTOF study were infected with 5×10^2 p.f.u. of WA1 and monitored for clinical signs of infection (for example, body weight and body temperature) starting from 1 to 9 days post-infection. CyTOF was conducted as described[29]. Single-cell suspensions of lung tissue specimens processed using the GentleMACS system (Miltenyi) were treated with 25 μM cisplatin (Sigma) for 60 s as a viability dye. Cells were then quenched with CyFACS buffer (PBS supplemented with 0.1% BSA and 0.1% sodium azide) and fixed for 10 min with 2% paraformaldehyde (PFA; Electron Microscopy Sciences). Cells were then washed twice with CyFACS buffer (PBS with 0.1% BSA, 0.05% sodium azide, and 2 mM EDTA) and frozen at −80 °C until CyTOF antibody staining. Before antibody staining, specimens were barcoded using the Cell-ID 20-Plex PD Barcoding kit (Fluidigm). Fc blocking was performed by treating the cells with 1.5% mouse and rat sera (both from Thermo Fisher) for 15 min at 4 °C. After washing with CyFACS, cells were stained for 45 min at 4 °C with the cell-surface antibodies listed in Extended Data Table 3. Antibodies were purchased pre-conjugated from Fluidigm or conjugated using the Maxpar X8 antibody labelling kit (Fluidigm). After staining, cells were washed with CyFACS and fixed overnight at 4 °C in 2% PFA and permeabilized for 30 min with Foxp3 fix/permeabilization buffer (Fisher Scientific). After two washes with permeabilization buffer (Fisher Scientific), cells were Fc blocked again for 15 min at 4 °C with mouse and rat sera diluted in permeabilization buffer. After washing with permeabilization buffer, cells were stained for 45 min at 4 °C with the intracellular antibodies listed in Extended Data Table 3. The details about the antibody dilutions have been provided in the Extended Data Table 3. Before CyTOF analysis, cells were incubated for 20 min with a 1:500 dilution DNA intercalator (Fluidigm), and then washed twice with CyFACS and once with Cell Acquisition Solution (CAS; Fluidigm). Acquisition was performed in the presence of EQ Four Element Calibration Beads (Fluidigm) diluted in CAS. Cells were analysed on a CyTOF 2 instrument (Fluidigm) at the UCSF Parnassus Flow Core. For data analysis, CyTOF datasets were normalized to EQ calibration using CyTOF software (6.7.1014, Fluidigm) and manually gated using the FlowJo software (10.7.2, FlowJo LLC, BD Biosciences). tSNE visualizations of the datasets were performed in Cytobank (9.1, 2022 Cytobank, Inc.), with default settings.

Histology

Mouse lung tissues were fixed in 4% PFA (47608, Sigma) for 24 h, washed three times with PBS and stored in 70% ethanol. In brief, tissues were processed and embedded in paraffin, and tissue sections were stained for SARS-CoV-2 nucleocapsid (GTX135357, Genetex). The sections were then imaged using Leica Aperio ImageScope.

Human serum samples

Human serum samples were acquired from two ongoing clinical trials led by Curative and the UCSF. The Curative clinical trial protocol was approved by Advarra under Pro00054108 for a study designed to investigate immune escape by SARS-CoV-2 variant (University of California, Los Angeles protocol record PTL-2021-0007; ClinicalTrials.gov identifier NCT05171803). Sample specimens were collected from adults (18–50 years of age) who either had been vaccinated for COVID-19 and/or had a history of COVID-19. Sample acquisition involved the standard venipuncture procedure to collect a maximum of 15 ml of whole blood, incubation at ambient temperature for 30–60 min to coagulate, centrifugation at 2,200–2,500 rpm for 15 min at room temperature, and storage on ice until delivered to the laboratory for serum aliquoting and storage at −80 °C until use. A quantitative SARS-CoV-2 IgG ELISA was performed on serum specimens (anti-SARS-CoV-2 ELISA (IgG), 2606–9621G, New Jersey, EuroImmun). Remnant plasma samples from patients hospitalized with COVID-19 at the UCSF were obtained from UCSF clinical laboratories daily, based on availability. Remnant samples were aliquoted and biobanked and the retrospective medical chart review for relevant demographic and clinical metadata were performed under a waiver of consent and according to 'no subject contact' protocols approved by the UCSF Institutional Review Board (protocol number 10-01116). Plasma samples were also collected through the UMPIRE (UCSF employee and community member immune response) study (protocol number 20-33083), a longitudinal COVID-19 research study focused on collection of prospective whole-blood and plasma samples from enrolled participants to evaluate the immune response to vaccination, with and without boosting, and/or vaccine breakthrough infection. The study cohorts included fully vaccinated individuals with either two doses of emergency use authorization-authorized mRNA vaccine (Pfizer or Moderna). Consented participants came to a UCSF CTSI Clinical Research Service (CRS) laboratory where their blood was drawn by nurses and phlebotomists. At each visit, two to four 3-ml EDTA tubes of whole blood were drawn, and one or two EDTA tubes were processed to plasma from each time point. Relevant demographic and clinical metadata from UMPIRE participants were obtained through participant Qualtric surveys performed at enrolment and at each blood draw. Serum samples were heat inactivated at 56 °C for 30 min before use in neutralization assays.

For adequate sample selection, the criteria were age, disease severity and days after infection for serum collection. A Wilcoxon–Mann–Whitney significance test was performed between the unvaccinated plus Omicron-infected and unvaccinated plus Delta-infected individuals, which showed no statistical significance in serum collection days after infection ($P = 0.147540$), disease severity index ($P = 0.820174$) and age of the individuals ($P = 0.591680$). A Wilcoxon–Mann–Whitney significance test was also performed between the vaccinated plus Omicron-infected and vaccinated plus Delta-infected individuals and showed no significant difference in serum collection days after infection ($P = 0.5267$) and age of the individuals ($P = 0.065$).

Reporting summary

Further information on research design is available in the Nature Research Reporting Summary linked to this paper.

Data availability

The datasets generated and/or analysed during the current study are available in the paper or in the Extended Data dataset.

27. Sachs, N. et al. Long-term expanding human airway organoids for disease modeling. *EMBO J.* **38**, e100300 (2019).
28. National Research Council, Division on Earth and Life Studies, Institute for Laboratory Animal Research & Committee for the Update of the Guide for the Care and Use of Laboratory Animals. *Guide for the Care and Use of Laboratory Animals: Eighth Edition* (National Academies Press, 2011).
29. Neidleman, J. et al. mRNA vaccine-induced T cells respond identically to SARS-CoV-2 variants of concern but differ in longevity and homing properties depending on prior infection status. *eLife* **10**, e72619 (2021).

Acknowledgements This research is funded by grants from the National Institutes of Health: NIH/NIAID (F31 AI164671-01) to I.P.C. and NHLBI U54HL147127 to M. Matthay. A.M.S. is supported by the Natural Sciences and Engineering Research Council of Canada (NSERC PDF-533021-2019). M.O. and W.C.G. also received support from the Roddenberry Foundation, from P. and E. Taft and the Gladstone Institutes. M.O. thanks Fast Grants and the Innovative Genomics Institute for support. J.A.D. acknowledges support from the National Institutes of Health (R21AI59666) and support from the Howard Hughes Medical Institute and the Gladstone Institutes. N.R.R. acknowledges support from the Van Auken Private Foundation, D. Henke, and Pamela and Edward Taft; and awards no. 2164 and no. 2208 from Fast Grants, which is part of Emergent Ventures at the Mercatus Center, George Mason University. C.Y.C. thanks the staff at the UCSF Clinical Laboratories and the UCSF Clinical Microbiology Laboratories for help in identifying and aliquoting nasal swab and plasma samples; and acknowledges support by the Innovative Genomics Institute at UC Berkeley and the UCSF, US Centers for Disease Control and Prevention contract 75D30121C10991, Abbott Laboratories and the Sandler Program for Breakthrough Biomedical Research at the UCSF. We thank S. Tamaki and C. Bispo for CyTOF assistance at the Parnassus Flow Core; the laboratory of E. Ghosn for guidance on lung cell processing; the Gladstone Histology Core; and the

James B. Pendleton Charitable Trust for support. The funders had no role in study design, data collection and analysis, decision to publish, or preparation of the manuscript.

Author contributions R.K.S., I.P.C. and M.O. conceptualized the study. R.K.S., I.P.C., T.M., A.M.S., C.R.S., A.C., M.M.K., B.S., P.-Y.C., R.G., C.-L.T. and A.F.G. performed the investigation. N.B., P.S., A.S.-G., V.S., A.G., J.N., I.S., B.M., N.K., V.H., M.S., L.L., M.B., F.T., F.W.S., C.Y.C. and L.S. performed the anti-sera collections. M.A.G.-K., M.K.M., D.W., C.H. and R.A. created the Omicron virus culture. X.F., M. Maishan and M. Matthay procured the lung tissue for organoids. M. Montano maintained the BSL3 facility. L.S., J.A.D., N.R.R., C.Y.C. and M.O. supervised the study. R.K.S., I.P.C. and M.O. wrote the original draft of the manuscript. R.K.S., I.P.C., G.R.K., W.C.G., T.M., N.R.R. and M.O. reviewed and edited the manuscript.

Competing interests J.A.D. is a cofounder of Caribou Biosciences, Editas Medicine, Scribe Therapeutics, Intellia Therapeutics and Mammoth Biosciences; a scientific advisory board member of Vertex, Caribou Biosciences, Intellia Therapeutics, eFFECTOR Therapeutics, Scribe Therapeutics, Mammoth Biosciences, Synthego, Algen Biotechnologies, Felix Biosciences, The Column Group and Inari; a director at Johnson & Johnson and Tempus; and has research projects sponsored by Biogen, Pfizer, AppleTree Partners and Roche. C.Y.C. is the director of the UCSF-Abbott Viral Diagnostics and Discovery Study; receives research support from Abbott Laboratories; and also receives support for SARS-CoV-2 research unrelated to this study from Mammoth Biosciences.

Additional information

Supplementary information The online version contains supplementary material available at https://doi.org/10.1038/s41586-022-04865-0.

Correspondence and requests for materials should be addressed to Nadia R. Roan, Charles Y. Chiu, Jennifer A. Doudna or Melanie Ott.

Peer review information *Nature* thanks Olivier Schwartz and the other, anonymous, reviewer(s) for their contribution to the peer review of this work.

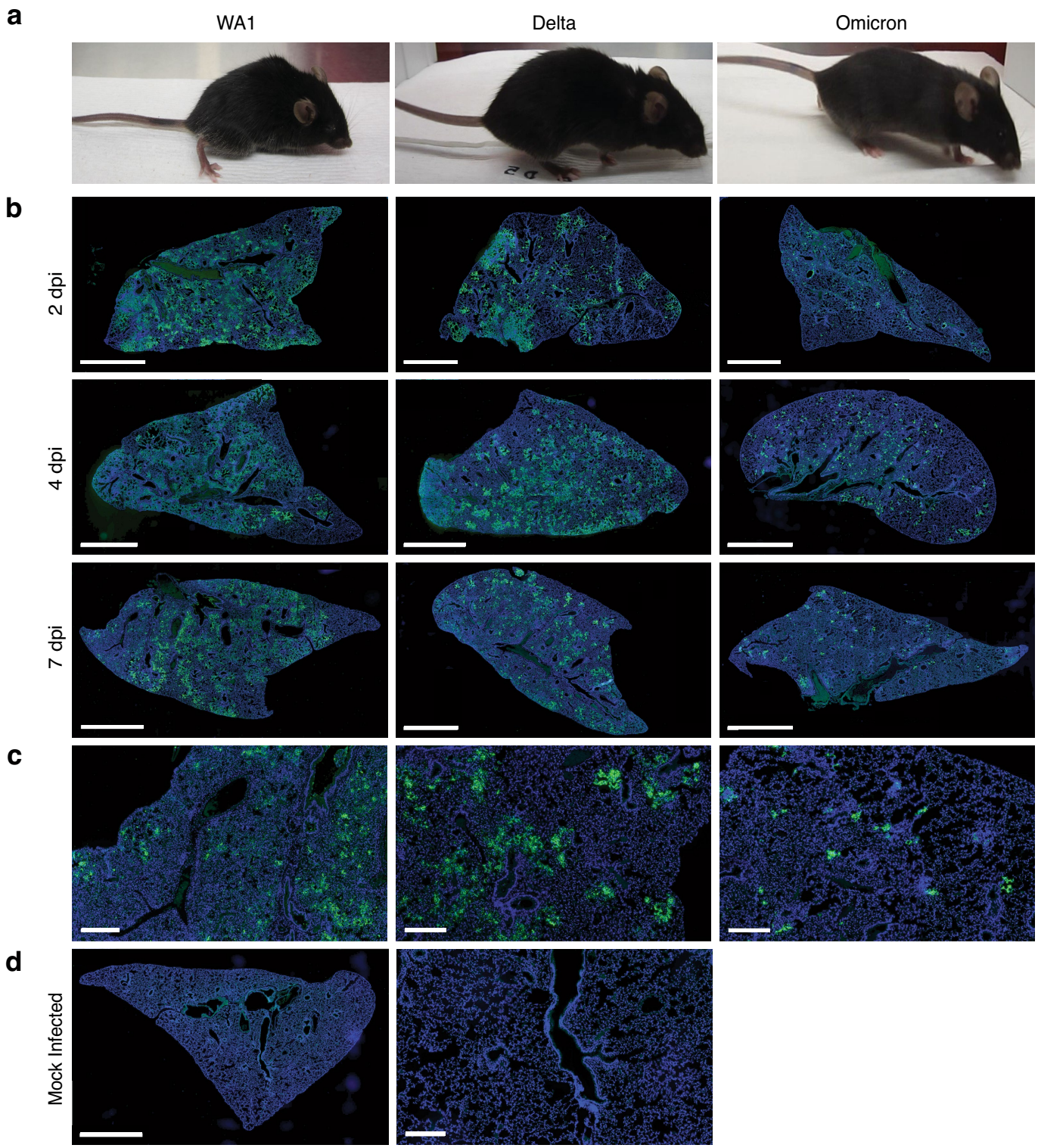

Extended Data Fig. 1 | Physical conditions of the infection mice at 5 dpi. **a**, Representative images of WA1-, Delta-, and Omicron-infected mice 5 dpi. WA1-infected mice were lethargic and had a hunched posture, ungroomed coat, and squinted eyes. Delta-infected mice are mildly lethargic. Omicron-infected mice appeared normal. **b**, Representative images of lungs from mice infected with WA1, Delta, or Omicron at 2 dpi (n = 5), 4 dpi (n = 5), and 7 dpi (WA1 infection group n = 2, Delta n = 2 and Omicron n = 5). SARS-CoV-2 nucleocapsid is stained in green and nucleus is stained in blue. Scale bar, 2 mm. **c**, Representative images of tissue sections from lung tissue infected with WA1, Delta, or Omicron collected at 7 dpi (WA1 infection group n = 2, Delta n = 2 and Omicron n = 5). SARS-CoV-2 nucleocapsid is stained in green and nucleus is stained in blue. Scale bar, 300 µm. **d**, Representative images of mock infected lungs. SARS-CoV-2 nucleocapsid is stained in green and nucleus is stained in blue. Scale bar, 2 mm (left panel) and 300 µm (right panel), n = 5 mice.

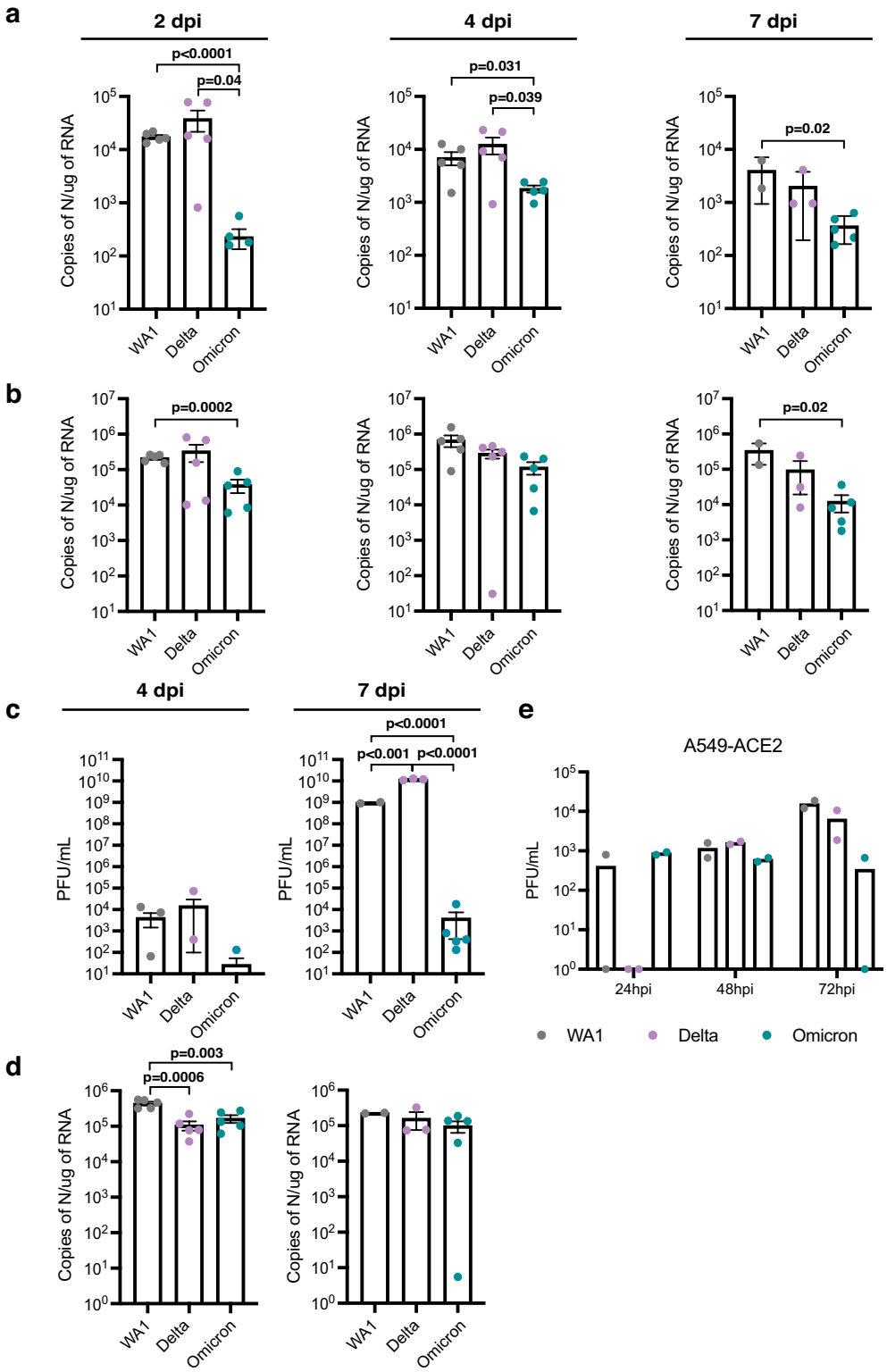

Extended Data Fig. 2 | Lower viral replication of Omicron in mice and human cells. a, RT-qPCR of SARS-CoV-2 N RNA isolated from upper respiratory tract (nasal turbinates and bronchus) of WA1-(grey), Delta-(purple), and Omicron-(teal) infected mice at indicated time points. Data are expressed in absolute copies/µg based on a standard curve of N gene with known copy number. Data are shown as an average ± SEM at 2 dpi (n = 5), 4 dpi (n = 5), and 7 dpi (WA1 infection group n = 2, Delta n = 2 and Omicron n = 5) and analyzed by two-tailed unpaired student's t-test. **b**, RT-qPCR of SARS-CoV-2 N RNA isolated from lungs of infected mice at indicated time points. Data are expressed in absolute copies/µg based on a standard curve of N gene with known copy number. Data are shown as an average ± SEM at 2 dpi (n = 5), 4 dpi (n = 5), and 7 dpi (WA1 infection group n = 2, Delta n = 2 and Omicron n = 5) and analyzed by the two-tailed unpaired student's t-test. **c**, Plaque assay titers from the brains of infected mice at indicated time points. Data are shown as an average ± SEM at 4 dpi (n = 5) and 7 dpi (WA1 infection group n = 2, Delta n = 2 and Omicron n = 5) and analyzed by the two-tailed unpaired student's t-test. **d**, RT-qPCR of SARS-CoV-2 N RNA isolated from brains of infected mice at indicated time points. Data are expressed in absolute copies/µg based on a standard curve of N gene with known copy number. Data are shown as an average ± SEM at 4 (n = 5) and 7 (n = 2–5) dpi and analyzed by the two-tailed unpaired student's t-test. **e**, Plaque assay titers from supernatants of infected A549-ACE2 (MOI of 0.01). Data are shown as average ± SEM, n = 2..

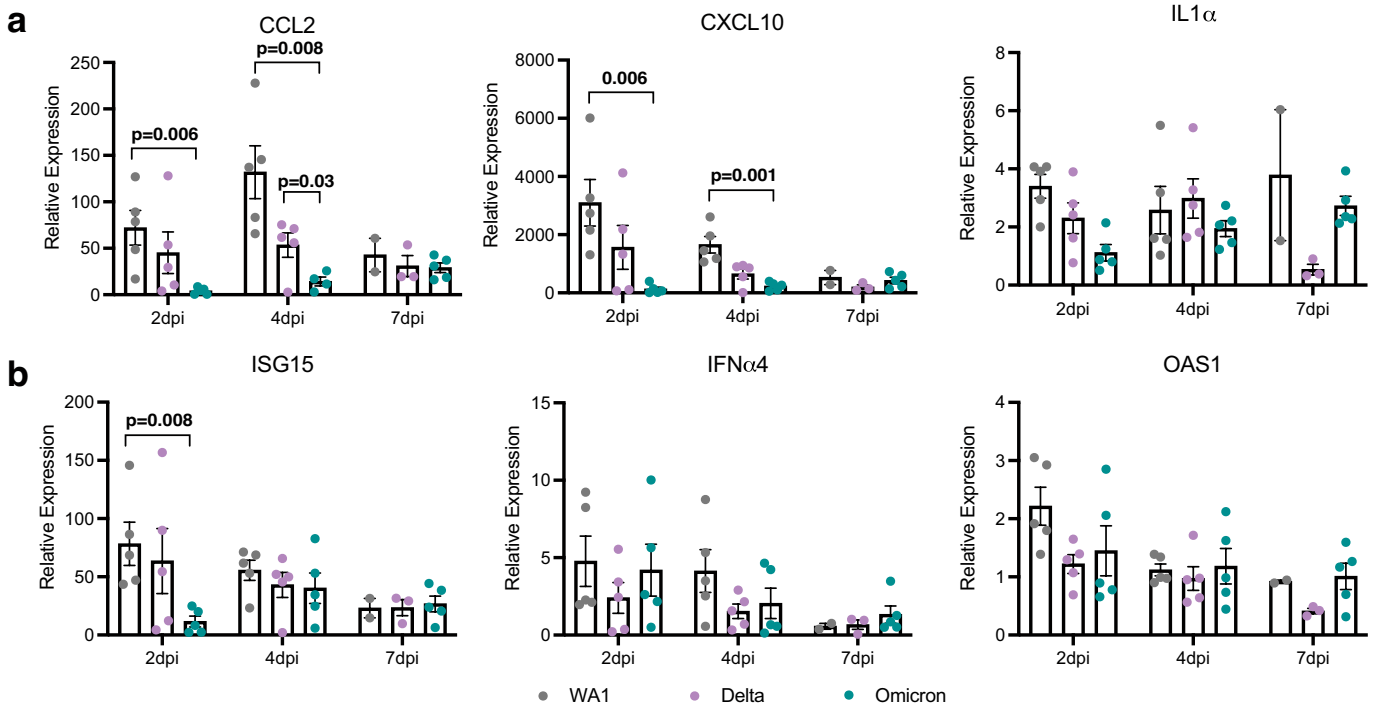

Extended Data Fig. 3 | Differential expression of proinflammatory markers in lungs of infected mice. a, RT-qPCR of proinflammatory cytokines and chemokines from RNA isolated from lungs of infected mice at the indicated time points. Data are expressed relative to mock-infected mice. Data are shown as the average ± SEM at 2 dpi (n = 5), 4 dpi (n = 5), and 7 dpi (WA1 infection group n = 2, Delta n = 2 and Omicron n = 5) and analyzed by two-tailed unpaired student's t-test. **b**, RT-qPCR of interferon-stimulated genes from RNA isolated from lungs of infected mice at the indicated time points. Data are expressed relative to mock-infected mice. Data are shown as the average ± SEM at 2 dpi (n = 5), 4 dpi (n = 5), and 7 dpi (WA1 infection group n = 2, Delta n = 2 and Omicron n = 5) and analyzed by the two-tailed unpaired student's t-test..

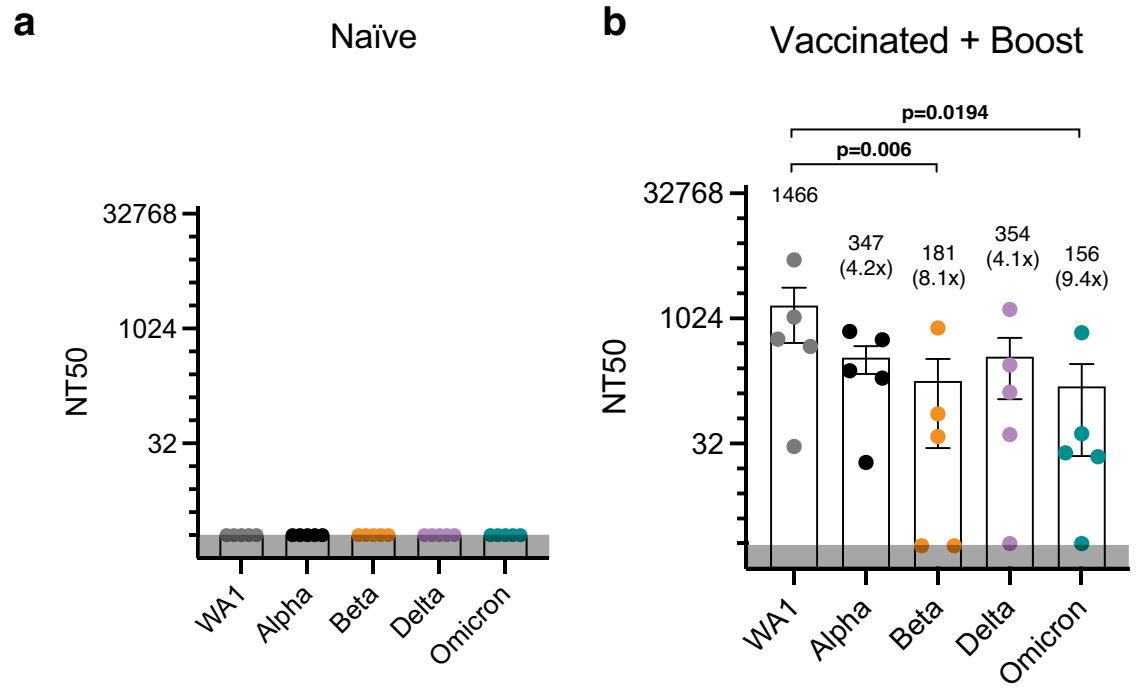

Extended Data Fig. 4 | Cross-variant neutralization of SARS-CoV-2 isolates by human sera. Graphs representing NT50 of sera from **a**, naive and **b**, vaccinated and Pfizer-boosted individuals against different viral isolates, n = 5 in each group. The average neutralization efficacies of sera from each graph are shown and fold-changes relative to ancestral isolate (WA1) are shown in parentheses. The grey band indicates the limit of detection. Data are shown as the average ± SEM and analyzed by 2-way ANOVA and adjusted for multiple testing using the Bonferroni test..

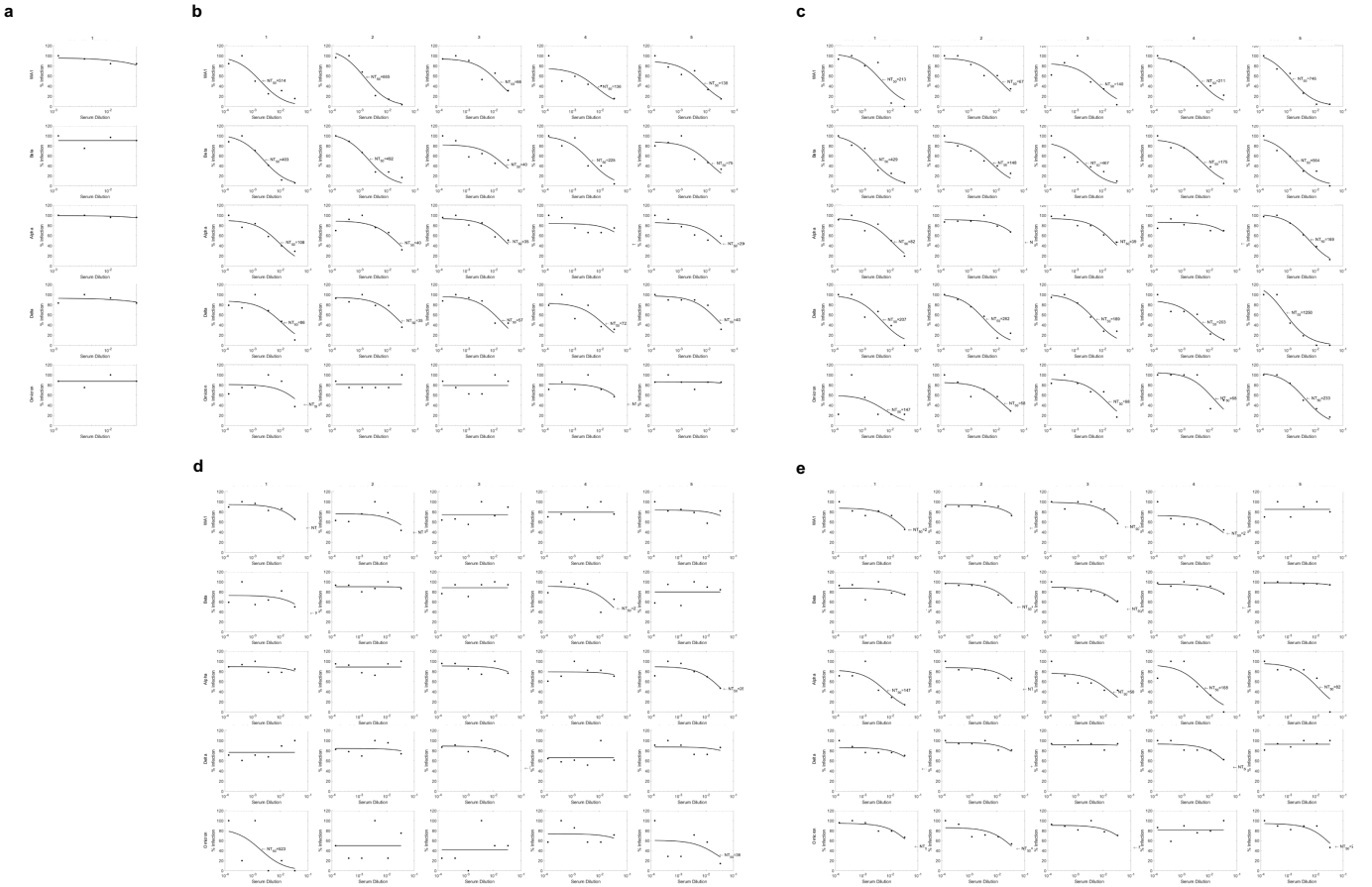

Extended Data Fig. 5 | Sera neutralizing titer assays of from SARS-CoV-2-infected mice. Neutralization assays of sera from **a**, naive (representative), **b**, WA1-, **c**, Delta-, and **d**, Omicron-infected mice at 7 days post-infection against WA1, Alpha, Beta, Delta, and Omicron isolates. **e**, Neutralization assays of sera from Omicron-infected mice at 9 days post-infection against WA1, Alpha, Beta, Delta, and Omicron isolates.

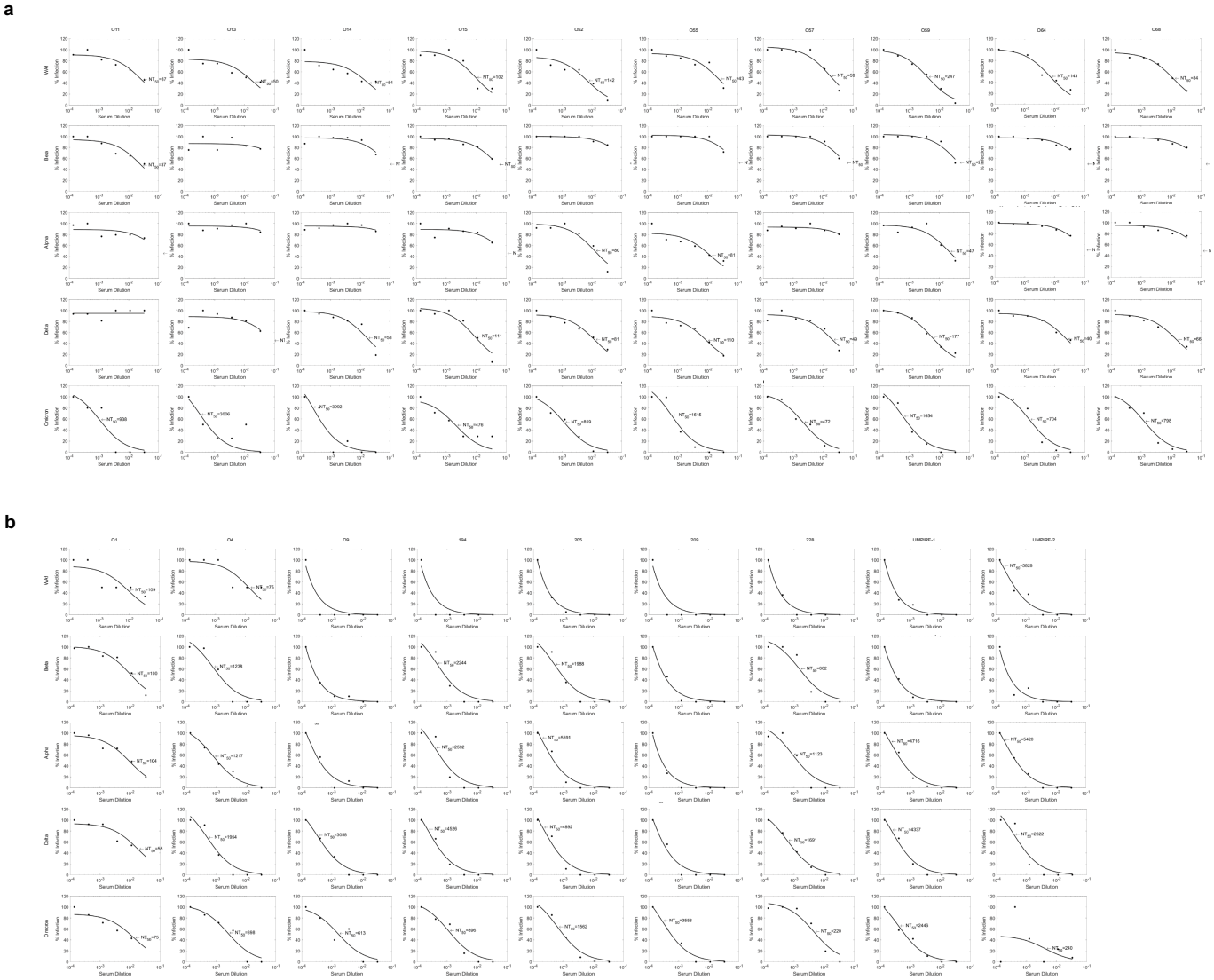

Extended Data Fig. 6 | Sera neutralizing titer assays of individuals infected with Omicron. Neutralization assays of sera from a, unvaccinated and b, vaccinated individuals infected with Omicron (likely based on time of collection) against WA1, Alpha, Beta, Delta, and Omicron isolates.

a

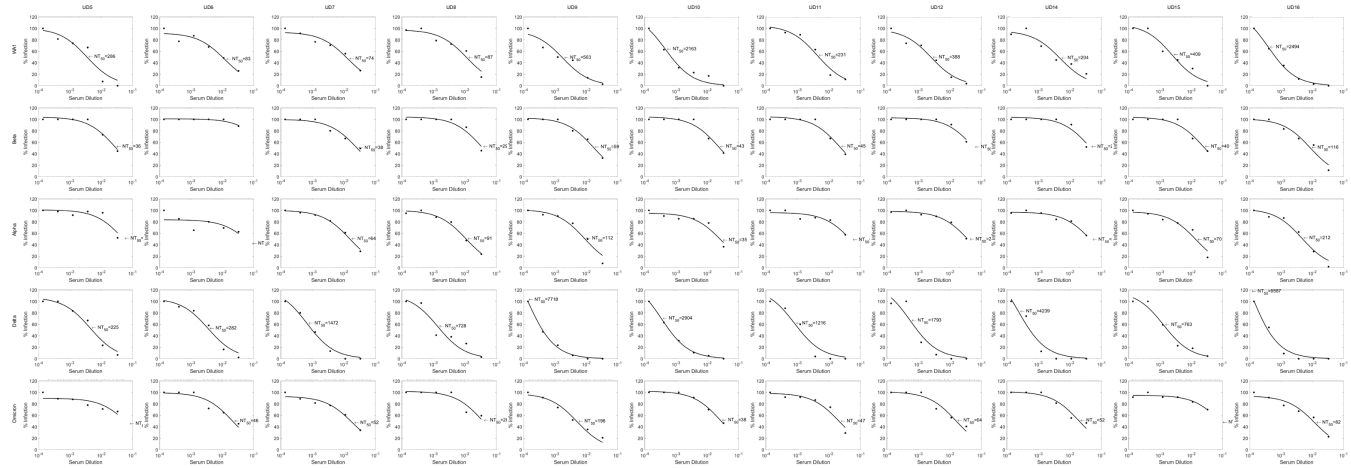

b

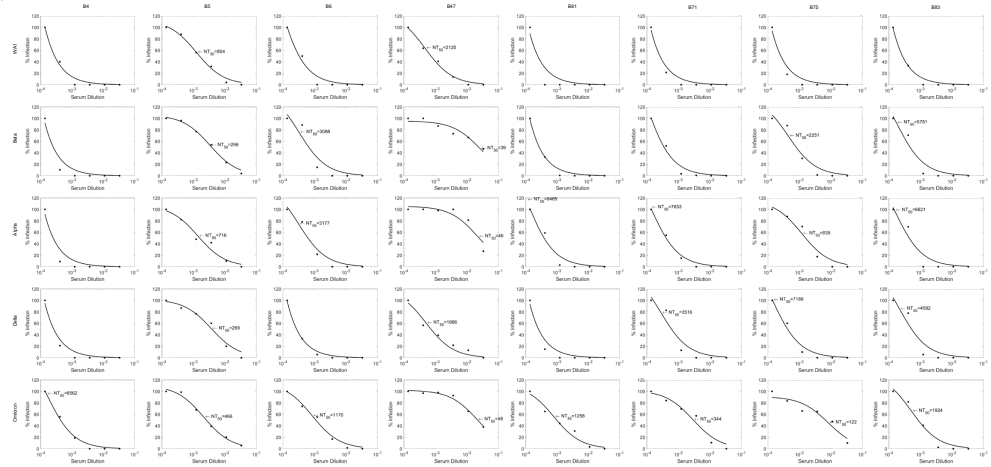

Extended Data Fig. 7 | Sera neutralizing titer assays from individuals infected with Delta. Neutralization assays of sera from **a**, unvaccinated and **b**, vaccinated individuals infected with Delta (likely based on time of collection) against WA1, Alpha, Beta, Delta, and Omicron isolates.

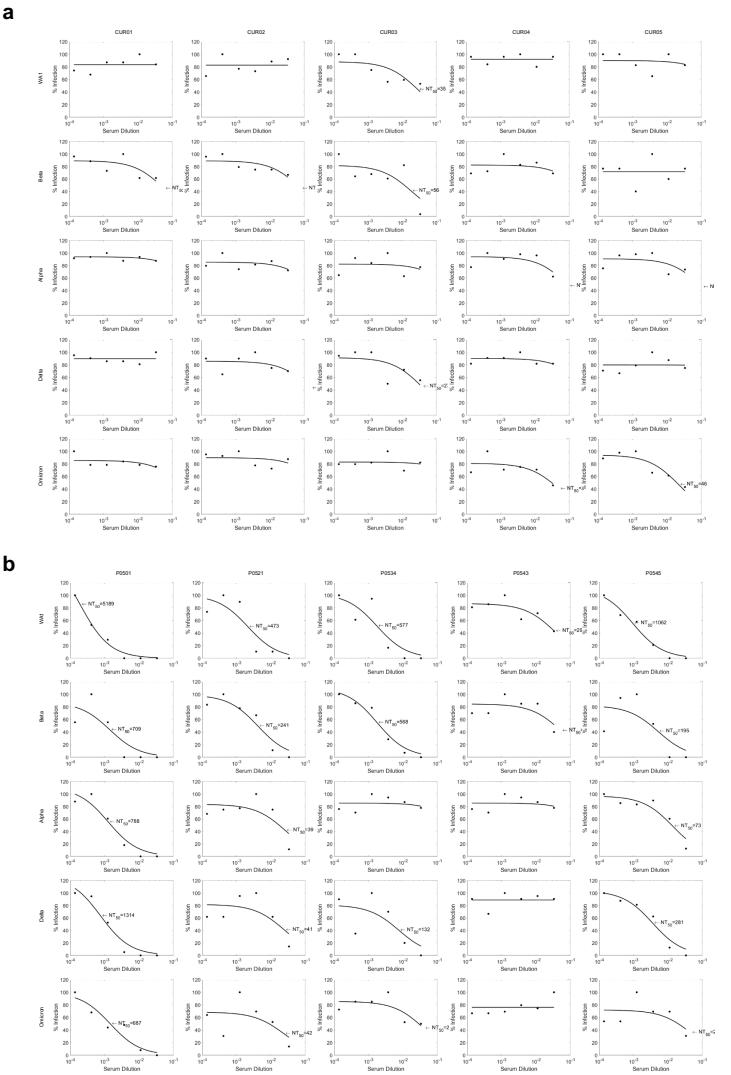

Extended Data Fig. 8 | Sera neutralizing titer assays from individuals. Neutralization assays of sera from **a**, naive and **b**, vaccinated and Pfizer boosted individuals against WA1, Alpha, Beta, Delta, and Omicron isolates.

Extended Data Table 1 | Clinical data of patients

Group	Patient ID	Age	Sex	Vaccine #1 date	Vaccine #1 manuf	Vaccine #2 date	Vaccine #2 manuf	Vaccine #3 date	Vaccine #3 manuf	Collection Date #1	Date COVID positive	Days after infection	Severity index
Naïve	CUR01	28	F	N/A	N/A	N/A	N/A	N/A	N/A	Not provided	N/A	N/A	N/A
	CUR02	65	M	N/A	N/A	N/A	N/A	N/A	N/A	Not provided	N/A	N/A	N/A
	CUR03	67	M	N/A	N/A	N/A	N/A	N/A	N/A	Not provided	N/A	N/A	N/A
	CUR04	26	F	N/A	N/A	N/A	N/A	N/A	N/A	Not provided	N/A	N/A	N/A
	CUR05	36	F	N/A	N/A	N/A	N/A	N/A	N/A	Not provided	N/A	N/A	N/A
Vaccinated + Boost	P0501	49	F	2/23/2021	Pfizer	3/23/2021	Pfizer	11/17/2021	Pfizer	12/1/2021	N/A	N/A	N/A
	P0521	52	M	2/23/2021	Pfizer	3/22/2021	Pfizer	10/4/2021	Pfizer	10/19/2021	N/A	N/A	N/A
	P0534	52	M	2/23/2021	Pfizer	3/23/2021	Pfizer	9/30/2021	Pfizer	10/15/2021	N/A	N/A	N/A
	P0543	48	M	2/23/2021	Pfizer	3/22/2021	Pfizer	10/8/2021	Pfizer	10/25/2021	N/A	N/A	N/A
	P0545	62	F	2/23/2021	Pfizer	3/22/2021	Pfizer	11/18/2021	Pfizer	12/3/2021	N/A	N/A	N/A
Vaccinated + Delta	B4	47	F	1/15/2021	Moderna	2/12/2021	Moderna	N/A	N/A	7/23/2021	7/18/2021	16	N/A
	B5	71	M	1/27/2021	Pfizer	2/17/2021	Pfizer	N/A	N/A	7/15/2021	7/14/2021	17	N/A
	B6	68	M	2/10/2021	Pfizer	3/12/2021	Pfizer	N/A	N/A	7/23/2021	7/22/2021	18	N/A
	B61	71	F	2/23/2021	Moderna	3/23/2021	Moderna	N/A	N/A	7/31/2021	7/31/2021	15	N/A
	B71	69	M	2/11/2021	Pfizer	3/4/2021	Pfizer	N/A	N/A	8/11/2021	8/11/2021	15	N/A
	B75	48	F	3/29/2021	Moderna	4/26/2021	Moderna	9/13/2021	Moderna	10/28/2021	10/30/2021	13	N/A
	B83	78	F	1/23/2021	Moderna	2/20/2021	Moderna	8/27/2021	Moderna	11/21/2021	11/18/2021	15	N/A
Vaccinated + Omicron	O4	28	F	8/22/2021	Pfizer	9/13/2021	Pfizer	Not provided	Not provided	1/5/2022	12/26/2021	11	N/A
	O6	81	F	1/29/2021	Moderna	3/5/2021	Moderna	11/10/2021	Moderna	1/13/2022	12/27/2021	18	N/A
	O7	70	M	3/25/2021	Pfizer	4/15/2021	Pfizer	N/A	N/A	12/28/2021	12/21/2021	8	N/A
	UMPIRE-1	30	M	3/10/2021	Pfizer	4/1/2021	Pfizer	10/7/2021	Pfizer	12/27/2021	12/17/2021	11	N/A
	194	39	F	3/29/2021	Moderna	4/26/2021	Moderna	N/A	N/A	2/10/2022	11/27/2021	75	N/A
	205	28	M	1/8/2021	Pfizer	1/31/2021	Pfizer	12/9/2021	Pfizer	2/15/2022	12/27/2021	48	N/A
	209	53	M	3/4/2021	Pfizer	4/4/2021	Pfizer	12/16/2021	Pfizer	2/8/2022	12/26/2021	44	N/A
	228	39	F	4/10/2021	Moderna	5/8/2021	Moderna	12/7/2021	Moderna	1/27/2022	12/28/2021	31	N/A
Unvaccinated + Omicron	O11	81	F	N/A	N/A	N/A	N/A	N/A	N/A	1/17/2022	12/30/2021	19	2
	O13	61	M	N/A	N/A	N/A	N/A	N/A	N/A	1/17/2022	12/31/2021	18	1
	O14	29	F	N/A	N/A	N/A	N/A	N/A	N/A	1/16/2022	1/6/2022	11	3
	O15	38	M	N/A	N/A	N/A	N/A	N/A	N/A	1/17/2022	1/4/2022	19	0
	O52	65	F	N/A	N/A	N/A	N/A	N/A	N/A	2/8/2022	1/24/2022	17	3
	O55	82	M	N/A	N/A	N/A	N/A	N/A	N/A	2/8/2022	1/19/2022	20	3
	O57	19	M	N/A	N/A	N/A	N/A	N/A	N/A	2/8/2022	1/18/2022	21	3
	O59	51	M	N/A	N/A	N/A	N/A	N/A	N/A	2/3/2022	1/17/2022	20	3
	O64	72	F	N/A	N/A	N/A	N/A	N/A	N/A	2/17/2022	1/30/2022	18	1
	O68	21	F	N/A	N/A	N/A	N/A	N/A	N/A	1/30/2022	1/16/2022	14	1
Unvaccinated + Delta	UD5	81	F	N/A	N/A	N/A	N/A	N/A	N/A	9/10/2021	9/5/2021	11	1
	UD6	81	F	N/A	N/A	N/A	N/A	N/A	N/A	10/27/2021	10/6/2021	21	1
	UD7	31	M	N/A	N/A	N/A	N/A	N/A	N/A	8/6/2021	8/4/2021	16	1
	UD8	100	F	N/A	N/A	N/A	N/A	N/A	N/A	10/6/2021	9/23/2021	16	2
	UD9	59	M	N/A	N/A	N/A	N/A	N/A	N/A	8/20/2021	8/1/2021	41	2
	UD10	25	F	N/A	N/A	N/A	N/A	N/A	N/A	8/13/2021	7/31/2021	15	2
	UD11	58	M	N/A	N/A	N/A	N/A	N/A	N/A	8/12/2021	7/6/2021	38	3
	UD12	57	F	N/A	N/A	N/A	N/A	N/A	N/A	8/13/2021	7/20/2021	24	3
	UD14	89	F	N/A	N/A	N/A	N/A	N/A	N/A	9/20/2021	8/31/2021	24	3
	UD15	32	M	N/A	N/A	N/A	N/A	N/A	N/A	10/7/2021	8/31/2021	37	3
	UD16	31	F	N/A	N/A	N/A	N/A	N/A	N/A	11/5/2021	10/12/2021	24	3

(N=46) included in the study. The human samples were acquired through clinical trials led by Curative Inc. and University of California, San Francisco (UCSF). F= Female, M= Male, N/A- Not applicable, severity index: 1-mild, 2-moderate, 3-severe.

Extended Data Table 2 | List of qPCR primers for mouse studies

Gene	Forward	Reverse
CCL2	CTTCTGGGCCTGCTGTTCA	CCAGCCTACTCATTGGGATCA
CXCL10	GCCGTCATTTTCTGCCTCAT	GCTTCCCTATGGCCCTCATT
IL1α	ACTGTTTCTAATGCCTTCCC	ATGGTTTCTTGTGACCCTGA
ISG15	GGCCACAGCAACATCTATGA	CGCAAATGCTTGATCACTGT
IFNα4	TCCATCAGCAGCTCAATGAC	AGGAAGAGAGGGCTCTCCAG
OAS1	ATTACCTCCTTCCCGACACC	CAAACTCCACCTCCTGATGC

The primers used to analyze cytokine expression in SARS-CoV-2- or mock-infected mice are listed.

Extended Data Table 3 | List of CyTOF-staining antibodies for mouse studies

Antibody	Clone	Metal label	Cat#	Vendor
Ly6G/C [Gr1]	RB6-8C5	141Pr	201306	Fluidigm
CD11c	N418	142Nd	201306	Fluidigm
CD69	H1.2F3	145Nd	104502	In-house
CD103	2E7	146Nd	121402	In-house
CD45	30-F11	147Sm	201306	Fluidigm
CD11b [MAC1]	M1/70	148Nd	201306	Fluidigm
CD19	6D5	149Sm	201306	Fluidigm
CD123	5B11	150Nd	106002	In-house
CD25	3C7	151Eu	101902	In-house
CD3e	145-2C11	152Sm	201306	Fluidigm
TER-119	TER119	154Sm	201306	Fluidigm
CXCR4	L276F12	159Tb	146502	In-house
CD62L	MEL-14	160Gd	104402	In-house
CD127	A7R34	161Dy	135029	In-house
CXCR5	L138D7	163Dy	145505	In-house
PD1	RMP1-30	164Dy	109113	In-house
CD8α	53-6.7	168Er	201306	Fluidigm
TCRβ	H57-597	169Tm	201306	Fluidigm
NK1.1	PK136	170Er	201306	Fluidigm
CD44	IM7	171Yb	201306	Fluidigm
CD4	RM4-5	172Yb	201306	Fluidigm
CD304	3E12	173Yb	145202	In-house
B220	RA3-6B2	176Yb	201306	Fluidigm
IL-5#	TRFK5	143Nd	201310	Fluidigm
IL-2#	JES6-5H4	144Nd	201310	Fluidigm
IL-21#	149204	155Gd	MAB594	In-house
Foxp3#	3G3	156Gd	MA5-16222	In-house
CTLA4#	UC10-4B9	157Gd	106302	In-house
IL-10#	JES5-16E3	158Gd	201310	Fluidigm
TNFα#	MP6-XT22	162Dy	201310	Fluidigm
IFNγ #	XMG1.2	165Ho	201310	Fluidigm
IL-4#	11B11	166Er	201310	Fluidigm
IL-6#	MP5-20F3	167Er	201310	Fluidigm
IL-17A#	TC11-18H10.1	174Yb	201310	Fluidigm
IFNα#	F18	175Lu	NB100-64387	In-house

#*Intracellular antibodies*

The table describes antibody reagents used to analyze the immune response in SARS-CoV-2- or mock-infected mice by CyTOF.

nature portfolio

Corresponding author(s): Melanie Ott, Jennifer Doudna, Charles Chiu, Nadia Roan

Last updated by author(s): Apr 29, 2022

Reporting Summary

Nature Portfolio wishes to improve the reproducibility of the work that we publish. This form provides structure for consistency and transparency in reporting. For further information on Nature Portfolio policies, see our Editorial Policies and the Editorial Policy Checklist.

Statistics

For all statistical analyses, confirm that the following items are present in the figure legend, table legend, main text, or Methods section.

n/a	Confirmed	
☐	☒	The exact sample size (*n*) for each experimental group/condition, given as a discrete number and unit of measurement
☐	☒	A statement on whether measurements were taken from distinct samples or whether the same sample was measured repeatedly
☐	☒	The statistical test(s) used AND whether they are one- or two-sided *Only common tests should be described solely by name; describe more complex techniques in the Methods section.*
☐	☒	A description of all covariates tested
☐	☒	A description of any assumptions or corrections, such as tests of normality and adjustment for multiple comparisons
☐	☒	A full description of the statistical parameters including central tendency (e.g. means) or other basic estimates (e.g. regression coefficient) AND variation (e.g. standard deviation) or associated estimates of uncertainty (e.g. confidence intervals)
☐	☒	For null hypothesis testing, the test statistic (e.g. *F*, *t*, *r*) with confidence intervals, effect sizes, degrees of freedom and *P* value noted *Give P values as exact values whenever suitable.*
☒	☐	For Bayesian analysis, information on the choice of priors and Markov chain Monte Carlo settings
☒	☐	For hierarchical and complex designs, identification of the appropriate level for tests and full reporting of outcomes
☒	☐	Estimates of effect sizes (e.g. Cohen's *d*, Pearson's *r*), indicating how they were calculated

Our web collection on statistics for biologists contains articles on many of the points above.

Software and code

Policy information about availability of computer code

Data collection	No software was used for data collection.
Data analysis	Data analysis was performed by using GraphPad Prism version 9.3. tSNE visualizations of the datasets were performed in Cytobank (9.1, 2022 Cytobank, Inc.), with default settings. CyTOF datasets were normalized to EQ calibration and manually gated using using CyTOF software (6.7.1014, Fluidigm) and manually gated using the FlowJo software (110.7.2, FlowJo LLC, BD Biosciences). NT50 graphs were generated by MATLAB (Version 9.12)

For manuscripts utilizing custom algorithms or software that are central to the research but not yet described in published literature, software must be made available to editors and reviewers. We strongly encourage code deposition in a community repository (e.g. GitHub). See the Nature Portfolio guidelines for submitting code & software for further information.

Data

Policy information about availability of data

All manuscripts must include a data availability statement. This statement should provide the following information, where applicable:

- Accession codes, unique identifiers, or web links for publicly available datasets
- A description of any restrictions on data availability
- For clinical datasets or third party data, please ensure that the statement adheres to our policy

The datasets generated during and/or analyzed during the current study are available in the manuscript or in the Extended data set.

Field-specific reporting

Please select the one below that is the best fit for your research. If you are not sure, read the appropriate sections before making your selection.

☒ Life sciences ☐ Behavioural & social sciences ☐ Ecological, evolutionary & environmental sciences

For a reference copy of the document with all sections, see nature.com/documents/nr-reporting-summary-flat.pdf

Life sciences study design

All studies must disclose on these points even when the disclosure is negative.

Sample size	For animal experiments, to estimate the minimum number of animals needed to reliably get the desired statistical significance ($p<0.05$) we performed power analysis and determined the animal number required for the experiment. Experiments with human samples: The human sera experiments contained samples from a total of 46 individuals divided in six groups with n value ranged between 5-11. A Wilcoxon-Mann-Whitney significance test was performed for criteria such as age, disease severity, and days after infection for serum collection to confirm the allocation of individuals between the groups are not statistically different. We confirmed that the sample size is well powered to answer questions in this research. Human organoid experiment: three individual experiments were performed from lung organoids generated from single human donor. The sample size was based on our previous experience of using Human organoids for SARS-CoV-2 infections.
Data exclusions	No data was excluded.
Replication	For animal experiments, we infected a group of five animals per group, per time point of the experiment and the experiment was repeated twice. The human lung organoid experiments were performed in triplicates. All attempts during replication of experiments were successful for all the experiments except for experiments involving patients samples which were analyzed once due to limited availability
Randomization	Randomization was not relevant to this study. For animal experiments: Animals were bred at Gladstone Institute with controlled and standardized housing and feeding conditions, Collection method of tissues or other samples was unified with covariates encoding gender and sample collection batches. Experiments using serum from human individuals: The participants were allocated based on criteria including age, disease severity, and days after infection for serum collection. A Wilcoxon-Mann-Whitney significance test was performed to confirm the allocation of individuals between the groups do not show statistical significance.
Blinding	For human individual samples the investigators were blinded to group allocation during data collection and/or analysis.

Reporting for specific materials, systems and methods

We require information from authors about some types of materials, experimental systems and methods used in many studies. Here, indicate whether each material, system or method listed is relevant to your study. If you are not sure if a list item applies to your research, read the appropriate section before selecting a response.

Materials & experimental systems

n/a	Involved in the study
☐	☒ Antibodies
☐	☒ Eukaryotic cell lines
☒	☐ Palaeontology and archaeology
☐	☒ Animals and other organisms
☐	☒ Human research participants
☐	☒ Clinical data
☒	☐ Dual use research of concern

Methods

n/a	Involved in the study
☒	☐ ChIP-seq
☒	☐ Flow cytometry
☒	☐ MRI-based neuroimaging

Antibodies

Antibodies used

Antibody, Clone, Metal label, Cat# ,Vendor
Ly6G/C [Gr1] RB6-8C5 141Pr 201306 Fluidigm
CD11c N418 142Nd 201306 Fluidigm
CD69 H1.2F3 145Nd 104502 In-house
CD103 2E7 146Nd 121402 In-house
CD45 30-F11 147Sm 201306 Fluidigm
CD11b [MAC1] M1/70 148Nd 201306 Fluidigm
CD19 6D5 149Sm 201306 Fluidigm
CD123 5B11 150Nd 106002 In-house

CD25 3C7 151Eu 101902 In-house
CD3e 145-2C11 152Sm 201306 Fluidigm
TER-119 TER119 154Sm 201306 Fluidigm
CXCR4 L276F12 159Tb 146502 In-house
CD62L MEL-14 160Gd 104402 In-house
CD127 A7R34 161Dy 135029 In-house
CXCR5 L138D7 163Dy 145505 In-house
PD1 RMP1-30 164Dy 109113 In-house
CD8α 53-6.7 168Er 201306 Fluidigm
TCRβ H57-597 169Tm 201306 Fluidigm
NK1.1 PK136 170Er 201306 Fluidigm
CD44 IM7 171Yb 201306 Fluidigm
CD4 RM4-5 172Yb 201306 Fluidigm
CD304 3E12 173Yb 145202 In-house
B220 RA3-6B2 176Yb 201306 Fluidigm
IL-5# TRFK5 143Nd 201310 Fluidigm
IL-2# JES6-5H4 144Nd 201310 Fluidigm
IL-21# 149204 155Gd MAB594 In-house
Foxp3# 3G3 156Gd MA5-16222 In-house
CTLA4# UC10-4B9 157Gd 106302 In-house
IL-10# JES5-16E3 158Gd 201310 Fluidigm
TNFα# MP6-XT22 162Dy 201310 Fluidigm
IFNγ # XMG1.2 165Ho 201310 Fluidigm
IL-4# 11B11 166Er 201310 Fluidigm
IL-6# MP5-20F3 167Er 201310 Fluidigm
IL-17A# TC11-18H10.1 174Yb 201310 Fluidigm
IFNα# F18 175Lu NB100-64387 In-house

Validation

Validated by manufacture and in-house.

Eukaryotic cell lines

Policy information about cell lines

Cell line source(s)

A549-ACE2 cell line from Synthego corporation was a gift from O. Schwartz, Vero-TMPRSS2 from S.P.J. Whelan. Vero-TMPRSS2-ACE2 were gifts from A. Creanga and B. Graham at NIH. 293T-ACE2-TMPRSS2 were generated in-house using 293T cells (CRL-3216) from ATCC.

Authentication

STR analysis and western blots were performed to confirm stable expression in cell lines.

Mycoplasma contamination

Annual mycoplasma contamination tests are performed on all cell lines and all the cell line were found negative for mycoplasma contamination.

Commonly misidentified lines
(See ICLAC register)

No commonly misidentified lines were used in current study.

Animals and other organisms

Policy information about studies involving animals; ARRIVE guidelines recommended for reporting animal research

Laboratory animals

B6.Cg-Tg(K18-ACE2)2Prlmn/J animals were bred at Gladstone institute animal facility. Female mice aged between 6–8-week-old were used for SARS-CoV-2 infection studies.

Wild animals

No wild animals were used in the study.

Field-collected samples

No field collected samples were used in the study.

Ethics oversight

All animals will be housed at AAALAC accredited ABSL3 facility of Gladstone Institutes. The experimental work will be carried out in accordance with the UCSF Institutional Animal Care and Use Committee (IACUC) and the recommendations of the Panel on Euthanasia of the American Veterinary Medical Association. All protocols concerning animal use were approved (AN169239-01C) by the Institutional Animal Care and Use committees at the University of California, San Francisco and Gladstone Institutes and conducted in strict accordance with the National Institutes of Health Guide for the Care and Use of Laboratory Animal (Council, 2011). Mice were housed in a temperature (65-75˚F) and humidity (40-60%) controlled pathogen-free facility with 12-hour light/dark cycle and ad libitum access to water and standard laboratory rodent chow.

Note that full information on the approval of the study protocol must also be provided in the manuscript.

Human research participants

Policy information about studies involving human research participants

Population characteristics

The human research participants (n=46) were characterized in six groups, including- Naive (n=5), Vaccinated + boost (n=5), Vaccinated + delta infected (n=7), vaccinated Omicron infected (n=8), unvaccinated + Omicron infected (n=10) and

	unvaccinated + Delta infected (n=11). All the information about the human research participants age, sex, COVID-19 infection status, vaccination dates, severity index and serum collection days after infection is provided in extended data table 1.
Recruitment	Human serum samples acquired from two ongoing clinical trials led by Curative and UCSF or from hospitalized patients at UCSF
Ethics oversight	1. Curative clinical trial protocol was approved by Advarra under Pro00054108. 2. UCSF Institutional Review Board approved protocol for remnant plasma samples obtained from patients hospitalized with COVID-19 at UCSF (protocol number 10-01116) and UCSF EMPloyee and community member Immune REsponse (protocol number 20-33083)

Note that full information on the approval of the study protocol must also be provided in the manuscript.

Clinical data

Policy information about clinical studies

All manuscripts should comply with the ICMJE guidelines for publication of clinical research and a completed CONSORT checklist must be included with all submissions.

Clinical trial registration	20-33083 (UCSF, protocol ID), NCT05171803 (Curative, ClinicalTrials.gov)
Study protocol	See Material and Methods.
Data collection	See Material and Methods.
Outcomes	See Material and Methods, trial ongoing.